



Exploring the utility of retinal optical coherence tomography as a biomarker for idiopathic intracranial hypertension: a systematic review

Mallika Prem Senthil¹ · Saumya Anand¹ · Ranjay Chakraborty¹ · Jose Estevez Bordon¹ · Paul A. Constable¹ · Shannon Brown² · Dalia Al-Dasooqi¹ · Simu Simon³

Received: 8 April 2024 / Revised: 24 May 2024 / Accepted: 26 May 2024 / Published online: 10 June 2024

© The Author(s) 2024

Abstract

This study aimed to examine the existing literature that investigated the effectiveness of optical coherence tomography (OCT) and optical coherence tomography angiography (OCT-A) as a biomarker for idiopathic intracranial hypertension (IIH). Our search was conducted on January 17th, 2024, and included the databases, Medline, Scopus, Embase, Cochrane, Latin American and Caribbean Health Sciences Literature (LILACS), International Standard Randomized Controlled Trial Number (ISRCTN) registry, and the International Clinical Trials Registry Platform (ICTRP). Our final review included 84 articles. In 74 studies, OCT was utilized as the primary ocular imaging method, while OCT-A was employed in two studies including eight studies that utilized both modalities. Overall, the results indicated that IIH patients exhibited significant increases in retinal nerve fiber layer (RNFL) thickness, total retinal and macular thickness, optic nerve head volume, and height, optic disc diameter and area, rim area, and thickness compared to controls. A significant correlation was observed between cerebrospinal fluid (CSF) pressure and OCT parameters including RNFL thickness, total retinal thickness, macular thickness, optic nerve head volume, and optic nerve head height. Interventions aimed at lowering CSF pressure were associated with a substantial improvement in these parameters. Nevertheless, studies comparing peripapillary vessel density using OCT-A between IIH patients and controls yielded conflicting results. Our systematic review supports OCT as a powerful tool to accurately monitor retinal axonal and optic nerve head changes in patients with IIH. Future research is required to determine the utility of OCT-A in IIH.

Keywords Idiopathic intracranial hypertension · Optical coherence tomography · Optical coherence tomography angiography · Retinal nerve fiber layer · Optic nerve head · Peripapillary vessel density

Introduction

Idiopathic intracranial hypertension (IIH) is a disorder of unknown etiology characterized by raised intracranial pressure (ICP) that predominantly affects obese women of childbearing age [1]. The prevalence of IIH in the general

population is 1–3 per 100,000 people but among women of childbearing age, the prevalence rate is higher at 5.5 per 100,000 [2–5]. The incidence of IIH has increased due to the rapid increase of obesity and the estimated total cost of IIH in the USA alone has exceeded USD \$444 million [6]. Although the exact cause of IIH is unknown, several theories have been postulated, including increased abdominal pressure, sleep apnea syndrome, reduction in cerebrospinal fluid (CSF) outflow or elevated venous sinus pressure [7–9]. The predominant symptom of IIH is headache, which can vary in intensity from mild to severe [10, 11] and chronic headache has been shown to significantly impact the quality of life of individuals with IIH [12, 13]. Other symptoms of IIH include tinnitus, visual obscuration, and diplopia [1, 10, 14, 15]. The accepted criteria for diagnosis of IIH includes the combination of raised

✉ Mallika Prem Senthil
mallika.premsthil@flinders.edu.au

¹ College of Nursing and Health Sciences, Caring Futures Institute, Flinders University, Bedford Park, Adelaide, South Australia 5042, Australia

² Central Library, Flinders University, Bedford Park, Adelaide, South Australia, Australia

³ University of Adelaide, Adelaide, South Australia, Australia

ICP without hydrocephalus or mass lesions, normal CSF composition, and normal neuroimaging [13]. There are currently no evidence-based guidelines for the medical and surgical management of IIH due to a lack of information on the efficacy of treatments and possible side effects [16, 17].

Chronic elevated ICP can lead to cerebral ischemia, cerebral edema, herniation, irreversible brain damage and in severe cases, death [18]. Hence, the precise measurement and continuous monitoring of ICP are crucial in caring for patients with IIH [19]. ICP can be accurately assessed using lumbar and transcranial methods but are invasive and carry an increased risk of bleeding and infection [20, 21]. Several non-invasive methods such as magnetic resonance imaging, computerized axial tomography imaging, transcranial doppler ultrasonography, tympanic membrane displacement, and ocular ultrasound have also been used to monitor the ICP changes in patients with raised IIH. However, these methods have limitations such as low sensitivity and specificity, poor inter-rater reliability, and poor test predictability [22]. Therefore, more accurate and reliable biomarkers are needed to evaluate the disease state.


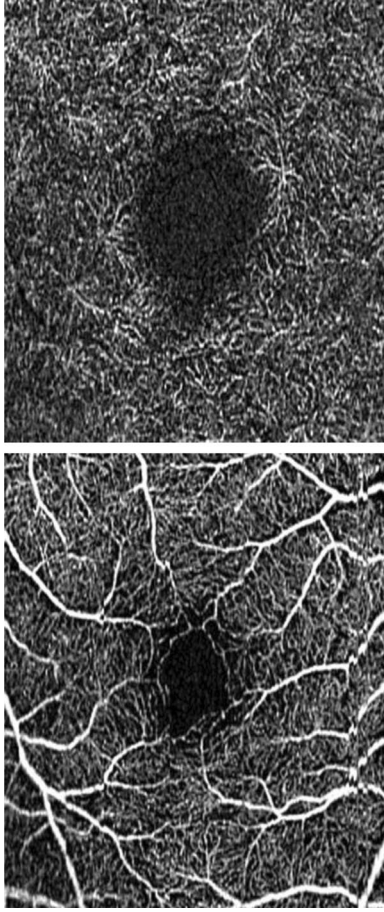
Optical coherence tomography (OCT) and optical coherence tomography angiography (OCT-A) are imaging modalities that provides qualitative and quantitative evaluation of the changes in the retinal nerve fibre layer (RNFL), optic nerve head, macula, and retinal and choroidal perfusion. While OCT can provide structural information about the retina and choroid, OCT-A provides information about the vasculature and blood flow of the retina and choroid (Table 1). OCT/OCT-A are routinely used in ophthalmic clinical settings to diagnose and monitor retinal conditions such as diabetic retinopathy, age-related macular degeneration, and retinal vascular occlusions [23–29]. OCT allows visualization of optic nerve head swelling, changes in the RNFL and retinal pigment epithelium/Bruch's membrane (RPE/BM) layer associated with acute and chronic changes in ICP. In addition, OCT-A allows the evaluation of vessel density on the optic disc and peripapillary region in both newly diagnosed and chronic IIH cases, making these imaging modalities valuable tools for both diagnosing and monitoring IIH [30, 31]. OCT can be useful to differentiate true disc edema, including papilledema from pseudoedema due to optic disc drusen. Studies have shown that RNFL thickness particularly in the nasal and inferior quadrants were reduced in optic disc drusen compared to optic disc edema [32, 33]. The standard for evaluating the severity of papilledema is the Frisén scale which grades the optic disc swelling from 0 to 5. Three-dimensional OCT parameters such as optic nerve head volume, height, and shape could potentially offer greater sensitivity compared to the Frisén scale in evaluating treatment outcomes among IIH patients [34]. This is because even in IIH patients with normal RNFL thickness, the optic

nerve head volume has been shown to be elevated [35]. The configuration of the RPE/BM layer in OCT scans can aid in distinguishing papilledema from disc edema caused by other factors like anterior ischemic optic neuropathy (AION). In papilledema, the RPE/BM layer exhibits a U-shape, angled toward the vitreous, whereas in AION and normal individuals, it assumes a V-shaped configuration, angled away from the vitreous [36, 37]. Increased ICP in IIH can cause biomechanical stress on the optic nerve head and retina resulting in retinal and choroidal folds, and OCT has been shown to be more sensitive than fundus photography is detecting these folds [38]. Quantitative assessments of vessel density surrounding the optic nerve head have shown a reduction in disorders such as optic neuritis, arteritic anterior ischemic optic neuropathy (AAION), and optic atrophy [39]. As such, the usefulness of OCT-A in diagnosing and monitoring IIH is still unclear. This systematic review examined the current body of literature regarding the utilization of OCT/OCT-A as a biomarker for IIH and reports the most suitable OCT/OCT-A parameters for the diagnosis and monitoring of IIH.

Methods

This systematic review followed the reporting guidelines outlined in the Preferred Reporting Items for Systematic reviews and Meta-Analyses (PRISMA) and was registered with the International Prospective Register of Systematic Reviews (PROSPER; ID: CRD42024520282). An initial search was performed using Medline and CINAHL to identify relevant articles and keywords. An extensive search strategy was then developed in Medline based on the identified keywords and index terms. The keywords used for the search included: “idiopathic intracranial hypertension”, “pseudotumor cerebri”, “pseudotumor syndrome”, “Nonne's syndrome”, “otitis hydrocephalus”, “benign intracranial hypertension”, “non-infective serous meningitis”. The retrieved articles from the Medline search were evaluated to confirm the inclusion of key publications. The search strategy, including the keywords and index terms, were adapted for other bibliographic databases such as PsycINFO (via Ovid SP), Latin American and Caribbean Health Sciences Literature (LILACS) and Scopus (Elsevier) (Online Resource 1). Each database search strategy was run on 17 January 2024. In addition, grey literature sources were searched including the International Standard Randomized Controlled Trial Number (ISRCTN) registry and the International Clinical Trials Registry Platform (ICTRP). There were no limits applied to language, but studies were excluded if they were solely animal studies, case report/case series, editorials, reviews, or conference abstracts. The primary outcome was to report the retinal and optic nerve head changes using OCT/OCT-A in IIH patients. Two authors (MPS and

Table 1 Comparison of optical coherence tomography (OCT) and optical coherence tomography angiography (OCT-A) imaging techniques

	Optical coherence tomography (OCT)	Optical coherence tomography angiography (OCT-A)
Key components	<p>It is a three-dimensional technique</p> <p>Optical coherence tomography uses infrared light directed toward the tissue under examination. The reflected light waves are then analyzed for time delay and differences in signal strength, which allows for assessment of tissue depth and imaging at the selected location</p> <p>The axial resolution of various OCTs is between 5 and 20 μm in the tissue</p>	<p>It is a three-dimensional technique</p> <p>Optical coherence tomography angiography uses low coherence interferometry with a focus on motion contrast of red blood cells for vascular imaging. The differences in the reflected OCT signal strength from consecutive OCT B-scans captured at the same location are used to generate an image of the blood flow</p> <p>The resolution of the instrument is 5–10 μm in the axial direction and ~20 μm in the transverse direction</p>
Strengths	<p>Cross-sectional retinal imaging providing detailed imaging of the retinal, choroidal, and optic nerve head structure</p> <p>Rapid image generation, with processing completed in seconds</p> <p>Non-invasive</p> <p>Portable</p>	<p>Detailed imaging of the retinal, choroidal, and optic nerve head vasculature and perfusion</p> <p>Quantitative imaging on vascular density and perfusion</p> <p>Rapid image generation, with processing completed in seconds</p> <p>Enables imaging of the retinal vascular flow without the need for injection of a dye</p> <p>Non-invasive</p> <p>Portable</p>
Limitations	<p>Inability to image blood flow</p> <p>Motion artifacts during imaging can lower the quality of the image</p>	<p>It lacks the ability to show vascular leakage</p> <p>Small field of view</p> <p>Presence of artifacts can hinder accurate interpretation of the image</p>
Image		

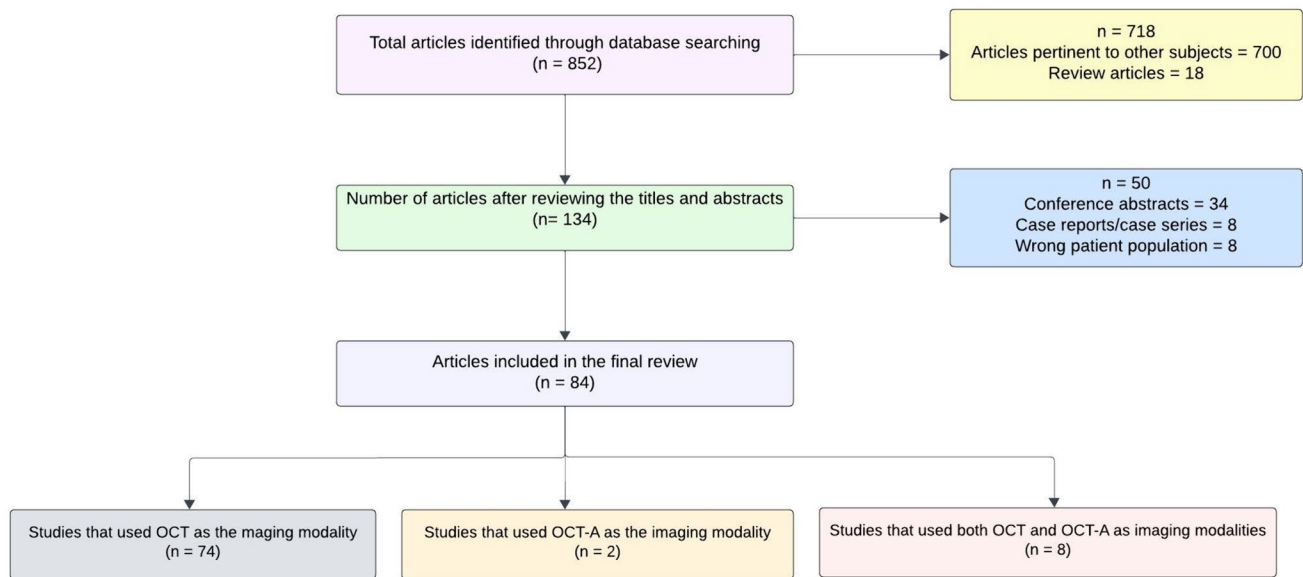


Fig. 1 Flow diagram of the systematic literature review search

JE) independently evaluated the titles and abstracts and then full-text reports for relevance utilizing Covidence (IBM, Detroit USA). Any discrepancies in the screening were resolved by mutual consensus between the authors. Reasons for exclusion of the studies were reported in each step of the review process. Included studies were assessed for quality according to the National Institutes of Health Quality Assessment Tool for observational cohort, case–control, cross-sectional, before–after studies with no control groups and controlled intervention studies. The assessment of case–control and before–after studies included 12 items scored as “yes”, “no”, or “other” (cannot determine, not applicable, not reported). The assessment of cohort, observational, and controlled intervention studies included 14 items that were again scored as “yes”, “no” or “other” (cannot determine, not applicable, not reported).

Results

Our initial search yielded 852 articles. Upon reviewing titles and abstracts, 718 articles were excluded (Fig. 1). After examining the full text of the remaining articles, an additional 50 were excluded. The final review comprised 84 articles that utilized ocular imaging as a biomarker for IIH (Table 2). We categorized the included articles into two groups: (1) studies employing OCT as the imaging technique in IIH, and (2) studies employing OCT-A as the imaging technique in IIH. The assessment of the risk of bias of the studies included in this review is shown in Online Resource 2.

Studies investigating OCT as the imaging modality in IIH

There were 82 studies that used OCT as an imaging modality in IIH. In these studies, OCT imaging was used to evaluate treatment effectiveness in patients with IIH, to compare the retinal and optic nerve head changes between IIH patients and healthy controls or to ascertain the relationship between OCT measurements and clinical parameters. The following OCT parameters were compared among the studies that reported them: peripapillary RNFL thickness [40–63], total retinal thickness [34, 64–71], macular thickness [72–75], macular ganglion cell complex (GCC) thickness [76–83], ganglion cell layer thickness [70, 84, 85], optic nerve head shape [30], optic nerve head volume [34, 35, 86–88], optic nerve head height [7, 35], optic nerve protrusion length [89], optic disc area [90, 91], optic disc diameter [92, 93], rim area [90, 91], rim thickness [50], optic cup volume [90], retinal folds [37, 94, 95], shape of peripapillary retinal pigment epithelium-basement membrane (ppRPE/BM) layer [7, 19, 30, 36, 96–98], anterior lamina cribrosa surface depth [99], posterior lamina cribrosa surface depth [99, 100], lamina cribrosa thickness [99, 100], Bruch’s membrane opening [69, 100], and pre-lamina tissue thickness (Figs. 2 and 3) [100]. The RNFL thickness was the OCT parameter most used in these studies [40, 43, 64, 66]. Most studies that compared the RNFL thickness between IIH patients and age-matched controls demonstrated that IIH patients had a significantly greater RNFL thickness compared to the controls [40, 43, 44, 51, 63, 64, 66, 101]. However, one study contradicted this trend, suggesting that control

Table 2 Summary of the studies included in the systematic review

Author	Year	Country	Study design	Sample size	Imaging	Device	Results
Rebolleda et al. [40]	2009	Spain	Case-control	IIH = 22 Controls = 22	OCT	Stratus OCT	The mean retinal nerve fibre layer (RNFL) and RNFL thickness in all quadrants in the eyes with papilledema were significantly greater than that of controls
Jensen et al. [64]	2010	Denmark	Case-control	IIH = 20 Controls = 20	OCT	Stratus OCT 3000	Baseline average RNFL and retinal thickness were significantly higher in patients with IIH compared to control
Scott et al. [65]	2010	USA	Cross-sectional	Papilledema = 36	OCT	OCT3	There was a significant correlation between OCT RNFL thickness, OCT total retinal thickness and modified Frisén scale (MFS) grades from photographs
Sinclair et al. [93]	2010	UK	Cross-sectional	IIH = 25	OCT	Stratus OCT	Elevation of the optic disc, diameter of the optic nerve sheath, and thickness of peripapillary RNFL significantly improved after weight loss
Sibony et al. [36]	2011	USA	Case-control	Papilledema = 25 AION = 20 Controls = 30	OCT	Cirrus OCT	The retinal pigment epithelium-basement membrane (RPE/BM) layer in controls and anterior ischemic optic neuropathy has a V-shape pointing away from vitreous. However, papilledema has a U shape pointing toward vitreous. Weight loss and shunting moved the U shape to V shape in papilledema patients
Skau et al. [136]	2011	Denmark	Case-control	IIH = 20	OCT	Stratus OCT 3000	Peripapillary OCT is a promising objective examination modality for optic disc evaluation in IIH and may improve the identification of subtle disc swellings
Skau et al. [66]	2011	Denmark	Case-control	IIH = 17 Controls = 20	OCT	Stratus OCT 3000	At baseline, average RNFL thickness and retinal thickness were significantly higher in IIH compared to controls. Changes in visual field mean deviation and pattern deviation from baseline to the final visit correlated significantly with OCT changes. During follow-up, patients improved significantly in OCT parameters and visual field sensitivity
Waisbourd et al. [41]	2011	Israel	Cross-sectional	IIH = 48	OCT	OCT3 3000	Average RNFL thickness was statistically different between the groups: the normal optic disc/mild elevation group, moderate elevation group, and the full-blown papilledema group
Kaufhold et al. [35]	2012	Germany	Case-control	IIH = 19 Controls = 19	OCT	Spectralis OCT	The 3D parameters, optic nerve head volume (ONHV), and optic nerve head height (ONHH) were able to discriminate between controls, treated, and untreated patients. Both ONHV and ONHH measures were related to levels of intracranial pressure (ICP)

Table 2 (continued)

Author	Year	Country	Study design	Sample size	Imaging	Device	Results
Yri et al. [67]	2012	Denmark	Case-control	IHH = 18 Controls = 20	OCT	Stratus OCT 3000	IHH patients with resolved papilledema at follow-up had a significant reduction in RNFL and retinal thickness values from 3-month follow-up visit to the final follow-up. At final follow-up, RNFL and retinal thickness were significantly thinner in IHH patients than healthy controls
Marzoli et al. [42]	2013	Italy	Cross-sectional	IHH = 38	OCT	RTVue-100 OCT	Mean average peripapillary retinal nerve fibre layer (ppRNFL) thickness was greater than normal values, while mean average macular ganglion cell complex thickness was lower than normal values
Skau et al. [43]	2013	Denmark	Case-control	IHH = 20 Controls = 20	OCT	Stratus OCT 3000	RNFL thickness was significantly increased in for all disc quadrants in newly diagnosed IHH
Auinger et al. [68]	2014	USA	Cross-sectional	IHH = 126 Controls	OCT	Cirrus OCT 4000	3D segmentation-based applications appear to be superior to commercially available 2D algorithms for calculating thickness of RNFL, total retinal thickness, and ganglion cell layer
Fard et al. [44]	2014	Iran	Case-control	Papilledema = 21 Pseudopapilledema = 19 Controls = 17	OCT	Spectralis OCT	RNFL thickness significantly increased in mild papilledema and pseudopapilledema compared to controls. Outer peripapillary total retinal volume is increased in only papilledema compared with pseudopapilledema and controls
Sibony et al. [19]	2014	USA	Pre-Post	IHH = 41 Controls = 30	OCT	Cirrus OCT	The ppRPE/BM changes with CSF pressure lowering interventions. Direct measurements of displacement at the basement membrane opening may serve as a more convenient office-based surrogate for shape analysis
Monteiro et al. [72]	2014	Brazil	Case-control	IHH = 29 Controls = 31	OCT	Cirrus OCT	The RNFL thickness and macular thickness significantly reduced in resolved papilledema compared to controls. Both measurements correlated with visual field sensitivity loss
OCT sub-study committee [34]	2015	USA	RCT	IHH = 89	OCT	Cirrus OCT 4000	RNFL thickness, total retinal thickness, and ONHV measurements improved with Diamox and weight loss
Chang et al. [89]	2015	USA	Case-control	IHH = 11 Controls = 11	OCT	Cirrus OCT	Mean OCT measurements of optic nerve protrusion length (NPL) were significantly larger than in controls. OCT and MRI measurements of NPL significantly correlated and significantly associated with Frisén papilledema grade

Table 2 (continued)

Author	Year	Country	Study design	Sample size	Imaging	Device	Results
Chen et al. [76]	2015	USA	Cross-sectional	IIH = 31	OCT	Cirrus OCT 4000	A ganglion cell layer-inner plexiform layer (GCL-IPL) thickness less than or equal to 70 μ m at initial presentation or progressive thinning greater than or equal to 10 μ m with 2–3 weeks compared with baseline correlated with poor visual outcome
Afonso et al. [137]	2015	Brazil	Case-control	PTC=24 Controls=26	OCT	3D OCT-1000	Both pattern electroretinogram (PERG) N95 amplitude and OCT parameters were able to discriminate papilledema eyes from controls with a similar performance. There was a significant correlation between PERG amplitude values and OCT parameters
Goldhagen et al. [73]	2015	USA	Case-control	IIH = 43 Controls = 30	OCT	Spectralis OCT	Total macular thickness was significantly thinner within the fovea and inner macular ring in non-trophic papilledema vs controls
Labib et al. [77]	2015	Egypt	Case-control	IIH = 30	OCT	RTVue SD-OCT	Initial RNFL thickness was significantly higher whereas macular ganglion cell complex (GCC) was significantly lower than controls. Macular GCC and RNFL thickness correlated with visual field loss
Moss et al. [78]	2015	USA	Case-control	IIH = 10 Controls = 15	OCT	Spectralis OCT	Photopic negative response was decreased in IIH patients and correlated with chronic ganglion cell injury and clinical measure of acute optic nerve head pathology
Sibony et al. [94]	2015	USA	Cross-sectional	IIH = 165 eyes	OCT	Cirrus OCT 4000	Folds are common in IIH and are three basic patterns: peripapillary wrinkles, retinal folds, and choroidal folds. OCT, specifically the raster and en face imaging, appears to be more sensitive in detecting folds than color fundus photography
Starks et al. [45]	2016	USA	Cross-sectional	IIH = 13	OCT	Stratus OCT	The visual field pattern deviation and RNFL are improved after optic nerve sheath fenestration
Dimkin et al. [46]	2017	USA	Pre-Post	IIH = 13	OCT	Cirrus OCT	Stenting of venous sinus stenosis is safe and results in reduction of ICP in IIH patients. This is associated with improvement in papilledema, RNFL thickness, visual field parameters and symptoms

Table 2 (continued)

Author	Year	Country	Study design	Sample size	Imaging	Device	Results
Gampa et al. [96]	2017	USA	Pre-Post	IIH = 20	OCT	Spectralis OCT	This study demonstrates a quantitative association between pp-BM shape and chronic ICP level. Changes in pp-BM shape is detectable within 1 h of lowering ICP. pp-BM shape may be a useful marker for chronic ICP level and acute ICP changes
Albrecht et al [86]	2017	Germany	Case-control	IIH = 21 Controls = 27	OCT	Spectralis OCT	In IIH, the ONHV increased and correlated with CSF pressure. The ONHV decreased after the initiation of treatment with Diamox
Kupersmith et al. [37]	2017	USA	Cross-sectional	IIH = 87	OCT	Cirrus OCT 4000	The various types of retinal folds associated with papilledema reflect biodynamic processes and show an acetazolamide treatment effect. Persistence of these folds, despite marked improvement in optic nerve head swelling, suggests permanent changes in the affected retinal tissues
Saenz et al. [47]	2017	USA	Cross-sectional	Papilledema = 23 Pseudopapilledema = 28	OCT	Cirrus OCT 4000	Compared to pseudopapilledema, papilledema eyes showed larger mean optic nerve sheath diameter, thicker RNFL
Wang et al. [30]	2017	USA	Cross-sectional	IIH = 125	OCT	Cirrus OCT 4000	Mean changes of the pRPE/BM shape measure were significant and in the positive direction (away from the vitreous) for the acetazolamide, but not for the placebo group
Aojula et al. [48]	2018	UK	Case-control	IIH = 46 Controls = 14	OCT	Spectralis OCT	Significantly greater thickness automated segmentation error (SegE) was present in RNFL thickness total area, assessed using ImageJ, in IIH patients compared to controls
Park et al. [79]	2018	USA	Case-control	IIH = 11 Controls = 11	OCT	Spectralis OCT	Mean full field photopic negative response (fPhNR) amplitude was reduced significantly in the patients compared to controls. The pattern pERG amplitude correlated significantly with Humphrey visual field mean deviation and GCC volume. However, the fPhNR amplitude was not correlated significantly with Humphrey visual field mean deviation or GCC volume
Sheils et al. [87]	2018	USA	Cross-sectional	IIH = 126 Controls	OCT	Cirrus OCT	Correlations between disc area and optic nerve head volume were similar in the treatment groups at baseline but were weaker in the acetazolamide group compared with the placebo group at 6 and 12 months in study eyes

Table 2 (continued)

Author	Year	Country	Study design	Sample size	Imaging	Device	Results
Banki et al. [97]	2019	USA	RCT	IIH = 165	OCT	Cirrus OCT 4000	The change in CSF pressure did not correlate with the change in IOP for either treatment group. There was no correlation between the CSF pressure and the optic nerve head (ONH) shape or CSF pressure-IOP pressure and ONH shape at baseline or at 6 months
Eren et al. [90]	2019	Turkey	Case-control	IIH = 54 Controls = 48	OCT	RTVue SD-OCT	The mean RNFL thickness was greater in the control group compared to IIH patients. The disc area, rim area was higher in the IIH group compared to controls, but the cup volume was lesser in the IIH group. There was a positive correlation between papilledema grade, rim area, RNFL thickness, CSF opening pressure, disc area, and rim area
Huang-Link et al. [49]	2019	Sweden	Case-control	IIH with papilledema = 8 IIH without papilledema = 9 Other neurological diseases = 19	OCT	Cirrus OCT 4000	IIH patients with papilledema had increased RNFL compared to IIH without papilledema and neurological diseases. RNFL reduced after CSF removal at 3 and 6 months in IIH patients with papilledema. However, no significant change in RNFL thickness after CSF removal was observed in IIH without papilledema or in patients with other neurological diseases
Onder et al. [50]	2019	Turkey	Cross-sectional	IIH = 18	OCT	Cirrus OCT 5000	There was a significant correlation between LP opening pressure and RNFL thickness. No association between RNFL measurements and MRI signs. Patients with IIH showed increased rim area and rim thickness but reduced optic cup volume
Pasaoglu et al. [99]	2019	Turkey	Case-control	IIH = 8 Controls = 10	OCT	Spectralis OCT	There was a significant difference in the anterior lamina cribrosa surface depth and the posterior lamina cribrosa surface depth between IIH patients and controls. No significant difference in lamina cribrosa thickness between IIH and controls
Merticariu et al. [51]	2019	Romania	Case-control	IIH = 11 Controls = 13	OCT	DRI Oct Triton	There was a significant difference in the average RFNL thickness between IIH and controls. There was also a correlation between papilledema severity and RNFL thickness
Wall et al. [52]	2019	USA	Case-control	IIH = 39 Controls = 98	OCT	Cirrus 5000 OCT	Although the presence of papilledema limited correlation, 55% of the temporal wedge defects had OCT RNFL deficits in the corresponding superonasal location

Table 2 (continued)

Author	Year	Country	Study design	Sample size	Imaging	Device	Results
Vijay et al. [88]	2020	UK	Cross-sectional	IIH = 104	OCT	Spectralis OCT	ONHV on OCT correlated with ICP. OCT can be used as a surrogate to inform ICP changes
Chen et al. [80]	2020	China	Cross-sectional	Primary PTCS = 9 Secondary PTCS = 46	OCT	Cirrus OCT	Secondary pseudotumor cerebri syndrome (PTCS) is more common than primary PTCS. OCT showed that eyes with intact macular GCL-IPL at baseline had good outcomes after treatment
Dreesbach et al. [103]	2020	Germany	Case-control	IIH = 21 Control eyes = 25	OCT	Spectralis OCT	ONHV was significantly increased in IIH compared to controls. The Frisén scale grading correlated higher with the ONHV than with RNFL thickness
Bahnasy et al. [53]	2020	Egypt	Cross-sectional	IIH with medical treatment = 59 IIH with LPS = 9	OCT	Spectralis OCT	Patients needed lumboperitoneal shunt showed statistically significant increase in baseline papilledema grade, mean deviation of visual field examination, optic nerve sheath diameter, average OCT–RNFL thickness, and P100 pattern reversal visual evoked potential latency. On the other hand, both studied groups showed statistically nonsignificant differences regarding the patients' ages and opening CSF pressure
Tatar et al. [100]	2020	Turkey	Case-control	IIH = 15 Controls = 17	OCT	EDI-OCT	Prelaminar tissue thickness and Bruch's membrane opening were significantly greater in IIH than controls. Anterior lamina cribrosa surface depth was significantly less in IIH than controls. No difference regarding lamina cribrosa thickness between IIH and controls
Orzdemir et al. [101]	2020	Turkey	Case-control	IIH = 22 Controls = 22	OCT	3D OCT-2000	IIH patients had increased RNFL thickness and choroidal thickness compared to controls. Subfoveal choroidal thickness was significantly correlated with ICP
Flowers et al. [54]	2021	USA	Cross-sectional	Papilledema = 22 Pseudopapilledema = 36	OCT	Cirrus OCT	The papilledema group had a higher mean RNFL thickness than the pseudopapilledema group
Nogueira et al. [81]	2021	Brazil	Case-control	IIH = 22 Controls = 11	OCT	RTVue-100	There was a significant association between macular GCC thickness and optic disc pallor and between edema and visual acuity. No significant difference was found in RNFL thickness between patients and controls. Macular GCC was thinner in patients with IIH compared to controls

Table 2 (continued)

Author	Year	Country	Study design	Sample size	Imaging	Device	Results
Bingol Kiziltuncet et al. [69]	2021	Turkey	Cross-sectional	IIH = 28	OCT	RTVue XR OCT	Bruch's membrane opening and maximal RNFL thickness were significantly higher in patients with increased CSF pressure. There exist correlations between CSF pressure and Bruch's membrane opening, maximal RNFL thickness and maximal retinal thickness. Bruch's membrane opening and maximal RNFL thickness can give an idea about increased CSF pressure values in IIH patients
Carey et al. [55]	2021	USA	Cross-sectional	IIH = 2 (20 scans)	OCT	Cirrus OCT	Multiple objective parameters of en face OCT of optic disc edema have an excellent correlation with ppRNFL thickness
Kabatas et al. [74]	2021	Turkey	Case-control	IIH = 56 Controls = 50	OCT	RTVue-XR 100 OCT	There was a significant difference in the mean RNFL thickness between IIH and controls. There was a significant positive correlation between the peripapillary RNFL thickness, the GCC thickness, and the CSF opening pressure. A similar result was also found between the Frisén grade and peripapillary RNFL
Kohil et al. [56]	2021	USA	Cross-sectional	Papilledema = 25 Pseudopapilledema = 24	OCT	Cirrus 5000 OCT	Ocular ultrasonography was 68% sensitive for papilledema and 54% specific for pseudopapilledema. Positive OUS correlated with elevated opening pressure on lumbar puncture and with signs of increased ICP on MRI
Panyala et al. [98]	2021	India	Case-control	Papilledema = 30 Papillitis = 30 Controls = 80	OCT	Cirrus OCT	97% of the eyes with papilledema had positive ppRPE/BM angle and 97% of the eyes with papillitis had negative ppRPE/BM angle. At 1 month, both RNFL thickness and ppRPE/BM reduced significantly in eyes with papilledema. RNFL normalized in 3 months and RPE/BM normalized in 6 months in patients with papilledema
Reggie et al. [95]	2021	USA	Cross-sectional	Papilledema = 32 Pseudopapilledema = 46	OCT	Cirrus 5000 OCT	Choroidal and/or retinal folds on OCT are commonly observed in patients with mild papilledema and are uncommon in those with pseudopapilledema
Touzé et al. [84]	2021	Canada	Cross-sectional	IIH = 16	OCT	Cirrus OCT	Mean RNFL was significantly decreased 1 month after stenting and at last visit. Ganglion cell thickness moderately decreased after stenting
Wibroe et al. [82]	2021	Denmark	Cross-sectional	IIH = 32	OCT	Spectralis OCT	The high prevalence of hyperreflective lines and peripapillary hyperreflective ovoid mass-like structures in IIH patients suggest these structures be a result of crowding in the optic nerve head caused by papilledema

Table 2 (continued)

Author	Year	Country	Study design	Sample size	Imaging	Device	Results
Banerjee et al. [138]	2022	India	Case-control	IIH = 27	OCT	Cirrus OCT 4000	At baseline, average RNFL had a moderate negative correlation with mean deviation and a positive correlation with log MAR visual acuity. Baseline GCL and log MAR visual acuity had a negative correlation. Optic disc height (ODH) had a negative correlation with visual field mean deviation. At 6 months, ODH and GCL-IPL complex had a statistically significant correlation with functional parameters
Inam et al. [57]	2022	USA	Cross-sectional	IIH = 53	OCT	SD-OCT	The mean changes in OCT RNFL and mean deviation in Humphrey visual field at 6 weeks were not different between low, medium, and high venous sinus pressure gradient
Jacobsen et al. [7]	2022	Norway	Case-control	IIH = 20 Controls = 12	OCT	Nidek's SD-OCT 3000	The peripapillary Bruch's membrane angle (pBA) and the ONHH differed between the IIH and reference groups and correlated with both mean ICP wave amplitude and mean ICP
Thaller et al. [58]	2022	UK	Cross-sectional	IIH = 123	OCT	SD-OCT	Increased weight gain during lockdown was associated with significant increase in papilledema (RNFL). RNFL thickness was reduced in patients with weight loss
Rehman et al. [91]	2022	India	Cross-sectional	IIH = 30	OCT	Cirrus OCT	A statistically significant change was observed in all OCT parameters during the 6-month follow-up (RNFL thickness, disc area, rim area, ONHV, mean retinal thickness, choroidal thickness)
Rehman et al. [75]	2022	India	Cross-sectional	IIH = 10	OCT	Cirrus OCT	Statistically significant difference in RNFL thickness and macular thickness in nasal quadrant was seen between the eyes with recurrence and without recurrence
Sood et al. [59]	2022	India	Cross-sectional	Optic disc edema = 64 (IIH = 10)	OCT	Cirrus OCT	The clinical severity of optic disc edema correlated positively with RNFL thickness, and most of the categories of optic disc edema followed the normative pattern of RNFL thickness (inferior > superior > nasal > temporal) despite thickening
Vosoughi et al. [60]	2022	Canada	Cross-sectional	IIH = 186	OCT	Cirrus 5000 OCT	Patients seeking care due to symptoms of IIH also had higher RNFL thickness, worse visual function, a higher, LP opening pressure, and worse final visual outcome
Attia et al. [70]	2023	France	Cross-sectional	IIH = 49 Intracranial tumors = 33 Cerebral venous thrombosis = 15	OCT	Spectralis OCT	Mean RNFL thickness and retinal thickness was significantly different between the optic atrophy and no atrophy group

Table 2 (continued)

Author	Year	Country	Study design	Sample size	Imaging	Device	Results
Kaya et al. [92]	2023	Turkey	Case-control	IIH = 43 Controls = 20	OCT	RTVue OCT	In the resolved-papilledema subgroup, peripapillary chorioidal thickness in all quadrants was significantly lower than in the control group. In the acute-papilledema subgroup, peripapillary chorioidal thickness in the temporal, inferior, and superior quadrants was significantly less than in the control eyes. The disc diameters in the vertical and horizontal planes was also significantly larger in the acute-papilledema eyes than in the control eyes and in the resolved papilledema eyes
Kaya Tutar et al. [61]	2023	Turkey	Cross-sectional	IIH = 21	OCT	Spectralis OCT	A statistically significant positive and moderate correlation was found between CSF pressure values and average RNFL thickness
Thaller et al. [139]	2023	UK	Cross-sectional	IIH = 490	OCT	Spectralis OCT	Those with the highest OCT RNFL had the worst visual outcomes
Thaller et al. [85]	2023	UK	Cross-sectional	IIH = 343	OCT	Spectralis OCT	OCT parameters did not differ significantly between symptomatic and asymptomatic disease
Xie et al. [62]	2023	Canada	Cross-sectional	IIH = 165	OCT	Cirrus OCT	Papilledema recurrence can be detected in atrophic optic discs using OCT
Bassi et al. [83]	2024	India	Cross-sectional	IIH = 20	OCT	SD-OCT	The RNFL thickness in all four quadrants had a weak positive correlation, and the GCL-IPL layer had a weak negative correlation with the ICP
Srija et al. [63]	2024	India	Case-control	Optic disc edema = 81 Controls = 74	OCT	Topcon 3D-OCT	Peripapillary RNFL thickness was significantly increased in the optic disc oedema group compared to controls
Wang et al. [71]	2024	USA	Case-control	IIH = 125 Controls = 96	OCT	Cirrus OCT	The montage colormaps of RNFL and total retinal thickness produced by the biVAE model provided an organized visualization of the variety of morphological patterns of optic disc oedema (including differing patterns at similar thickness levels)
Yalcinkaya Cakir et al. [108]	2023	Turkey	Case-control	IIH = 30 ODD = 33 Controls = 70	OCT & OCT-A	Topcon	Peripapillary vascular density is reduced in patients with IIH and optic disc drusen (ODD) compared to healthy controls. There is a significant difference in the vascular density in deep capillary plexus and choriocapillaris between IIH and ODD

Table 2 (continued)

Author	Year	Country	Study design	Sample size	Imaging	Device	Results
Fard et al. [110]	2019	Iran	Case-control	Papilledema = 21 Pseudopapilledema = 15 Controls = 44	OCT & OCT-A	AngioVue	Average RNFL was greater in patients with papilledema compared to pseudo and controls. No difference in GCC thickness between the three groups. Peripapillary vasculature values were significantly lower in papilledema and pseudo compared to controls
Rodriguez Torres et al. [140]	2021	USA	Cross-sectional	IIH = 23	OCT & OCT-A	AngioVue	Skeletonized vessel density peripapillary capillary plexus was significantly associated with papilledema grades, RNFL thickness, GCL thickness. Increased grading was associated with decrease of vessel density
El-Haddad et al. [141]	2023	Egypt	Cross-sectional	IIH = 21	OCT-A	AngioVue	Optic disc vessel density decreased after shunt surgery in patients with IIH. There were positive correlations between the CSF opening pressures and the preoperative optic disc vessel density of the whole image and inside disc. In addition, there was a positive correlation between the opening CSF pressures and the reduction in whole image vessel density after surgery
Wang et al. [111]	2023	China	Case-control	IIH = 61 Controls = 65	OCT & OCT-A	VG200S, Svision	Patients with IIH showed thicker ppRNFL and GCL-IPL thickness with larger ONH rim area when compared to controls. Microvascular densities were increased in nerve fibre layer plexus while densities were reduced in superficial vascular plexus, intermediate capillary plexus, and deep capillary plexus compared to controls
Pahuja et al. [102]	2023	India	Case-control	IIH = 41 Controls = 10	OCT & OCT-A	Angioplex	RNFL thickness showed significant thinning in the early, chronic, and atrophic papilledema. GC-IPL was significantly reduced in all groups compared to controls
Kwapong et al. [113]	2023	China	Case-control	IIH = 46 Controls = 42	OCT & OCT-A	VG200S, Svision	Compared with the control group, IIH patients showed reduced microvascular densities and thinner retinal thicknesses. ICP correlated with the microvascular densities and GCL-IPL thickness in IH patients for superficial vascular complex and deep vascular complex
Chonsui et al. [112]	2022	France	Cross-sectional	Papilledema = 20 Controls = 33	OCT & OCT-A	PLEX Elite	There was a decreased peripapillary capillary density without changes in capillary flux intensity (CFI) in eyes with papilledema. There were a positive association between the CFI and the RNFL and a negative association between the capillary perfusion density (CPD) and the RNFL

Table 2 (continued)

Author	Year	Country	Study design	Sample size	Imaging	Device	Results
Kaya et al. [109]	2021	Turkey	Case-control	IIH = 31 Controls = 52	OCT-A	AngioVue	The vessel density in the inferior nasal region in IIH patients significantly exceeded the vessel density of the controls. RNFL and GCC thickness were comparable between IIH and controls
Tüntaş Bilen et al. [107]	2019	Turkey	Case-control	IIH = 19 Controls = 21	OCT & OCT-A	AngioVue	There was a decrease in peripapillary density in patients with IIH compared to health controls

RCT randomized controlled trial; *IIH* idiopathic intracranial hypertension; *AION* anterior ischemic optic neuropathy; *PTC* pseudotumor cerebri; *PTCS* pseudotumor cerebri syndrome; *LPS* lumbo-peritoneal shunt; *ODD* optic disc drusen; *OCT* optical coherence tomography; *OCT-A* optical coherence tomography angiography; *CSF* cerebrospinal fluid; *ICP* intracranial pressure

subjects had higher RNFL thickness compared to those with IIH, while another study found no significant difference in RNFL thickness between IIH patients and controls [81, 90]. In addition, it was observed that that IIH patients had initially thicker RNFL measurements, which gradually decreased over subsequent follow-up periods at 1, 3, 6, and 12 months [34, 40, 66, 67]. Among the IIH patients, those with severe papilledema were shown to have thicker RNFL than in patients with normal optic discs/minimally or moderately raised discs [41]. Patients with recurrent IIH and those without recurrence of IIH were found to have significantly different RNFL thicknesses, with the recurrence group reported to have thicker neural tissue [91]. Similarly, RNFL was greater in papilledema than in pseudopapilledema patients [54]. However, the RNFL thickness did not differ between the symptomatic and asymptomatic groups [85]. Compared to healthy controls, patients with chronic and atrophic papilledema had significantly thinner RNFL thickness [102]. In OCT imaging, ppRPE/BM is seen as a well-defined layer above the choroid in the outer retina. It is V-shaped and angled away from the vitreous in normal individuals (Fig. 4). However, in IIH patients with raised ICP, it is U-shaped and angled toward the vitreous (Fig. 5) [36, 98]. Interventions aimed at lowering the CSF pressure such as lumbar puncture and CSF shunt have demonstrated an ability to transform the ppRPE/BM layer from a U-shaped configuration to the more typical V-shaped configuration [19, 30, 36].

Few studies used a custom segmentation algorithm to develop 3D parameters such as optic nerve head volume and optic nerve head height to compare the optic nerve head changes between IIH patients and controls. They showed that the optic nerve head volume and optic nerve head height were increased in IIH patients than in controls [35, 103]. In addition, optic nerve head volume was used to differentiate between controls, treated, and untreated patients with IIH [35]. Optic disc area, diameter, rim area, thickness, and Bruch's membrane opening were reported to be thicker in IIH patients compared to controls [69, 90]. In contrast, individuals with IIH exhibited thinner macular GCC, diminished thickness of the peripapillary choroid, reduced depth of both the anterior and posterior lamina cribrosa surfaces depths, and a decrease in optic cup volume [42, 77, 81, 90, 99]. OCT imaging was also shown to be sensitive in detecting folds such as peripapillary wrinkles, retinal and choroidal folds in patients with IIH [95].

Studies that investigated the utility of OCT in evaluating treatment outcomes in IIH patients demonstrated a significant improvement in the OCT parameters (RNFL thickness, total retinal thickness, choroidal thickness, optic nerve head volume, rim, and disc area) after interventions such as weight loss, oral acetazolamide, and optic nerve sheath fenestration [45, 86, 91]. Studies that examined the relationship

Fig. 2 Optical coherence tomography (OCT) image of the retina showing the different layers. *ILM* inner limiting membrane; *RNFL* retinal nerve fiber layer; *GCL* ganglion cell layer; *INL* inner nuclear layer; *IPL* inner plexiform layer; *ONL* outer nuclear layer; *OPL* outer plexiform layer; *ELM* external limiting membrane; *RPE* retinal pigment epithelium. Macular thickness = distance between ILM and RPE; retinal thickness = distance between ILM and photoreceptor layer; choroidal thickness = distance between the outer border of RPE and choroidoscleral surface

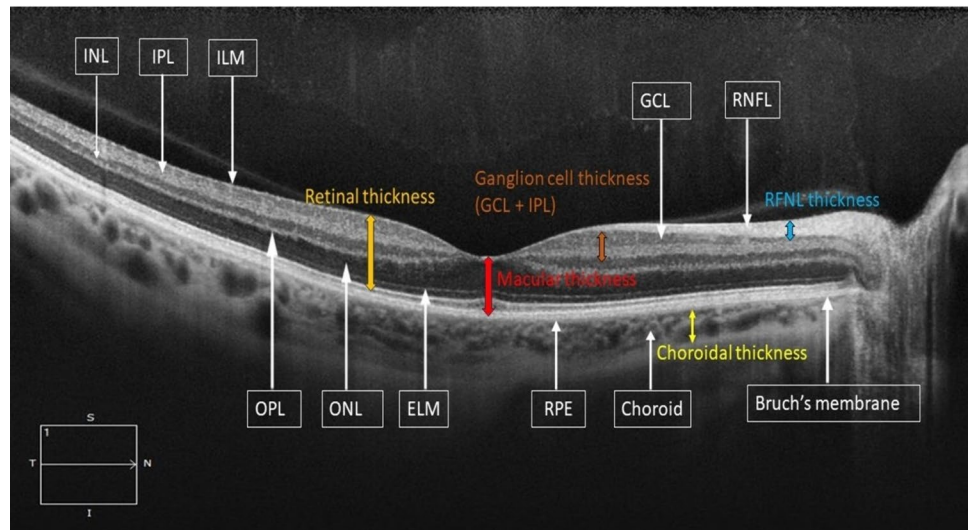
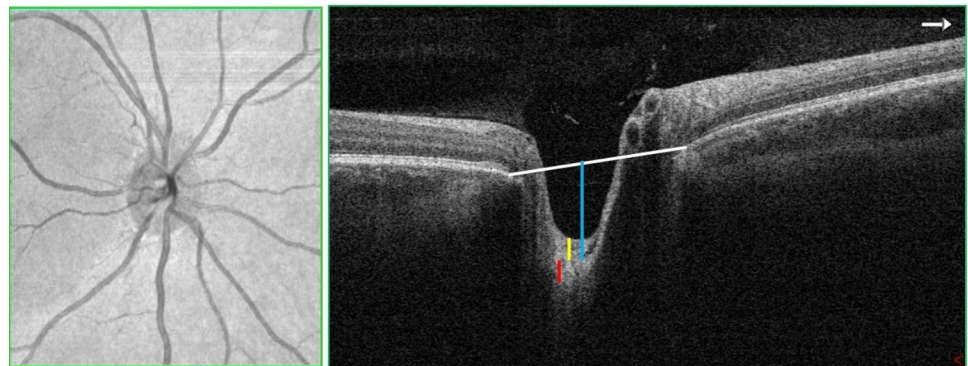


Fig. 3 Optical coherence tomography (OCT) imaging of the optic disc. The white line is Bruch's membrane opening, the blue line is lamina cribrosa surface depth, the yellow line is pre-laminar tissue thickness, and the red line is lamina cribrosa thickness



between OCT measurements and clinical parameters showed a significant positive correlation between CSF pressure and various OCT parameters, including RNFL thickness, retinal thickness, macular GCC, optic nerve head volume, optic nerve head height, ppRPE/BM layer and Bruch's membrane opening [35, 50, 51, 59, 61, 69, 86]. RNFL thickness showed significant positive correlation with visual acuity, visual field loss, papilledema severity, and the Modified Frisén Scale (MFS grades) from fundus photographs [40, 65, 77]. In addition, macular GCC thickness was found to be significantly associated with optic disc pallor [81]. However, no association was identified between CSF pressure and the shape of the optic nerve head [97].

Studies investigating OCT-A as the imaging modality in IIH

Ten studies explored the applicability of OCT-A as a non-invasive imaging biomarker for IIH. In these studies, OCT-A examinations were primarily done in acute settings of papilledema except two studies in chronic papilledema settings. Most of these studies employed OCT-A to assess the

peripapillary vascular density differences between individuals with IIH and control groups. The peripapillary area is a ring-shaped zone extending from the optic disc boundary (Fig. 4) [104]. Vessel density is defined as the percentage of area occupied by both large vessels and microvasculature in a specific area and is calculated over the entire scan area, as well as in the defined sectors within the scan [105]. Capillary flux intensity is defined as the total weighted area of perfused microvasculature per unit area and capillary perfusion density is defined as the total area of perfused microvasculature per unit area. The retinal vascular network is organized into four distinct plexuses: the superficial capillary plexus (SCP), intermediate capillary plexus (IP), deep capillary plexus (DCP), and radial peripapillary capillary plexus (RPC) [106]. The central retinal artery supplies blood to the SCP which then anastomoses and creates the IP and the DCP. The SCPs are located with the RNFL, ganglion cell layer, and the inner plexiform layer and the DCPs are located within the outer plexiform layer below the IP. The RCP, however, runs parallel with the nerve fiber layer axons (Fig. 5).

Several studies have investigated the peripapillary vessel density in patients with IIH in comparison to controls. Tuntas

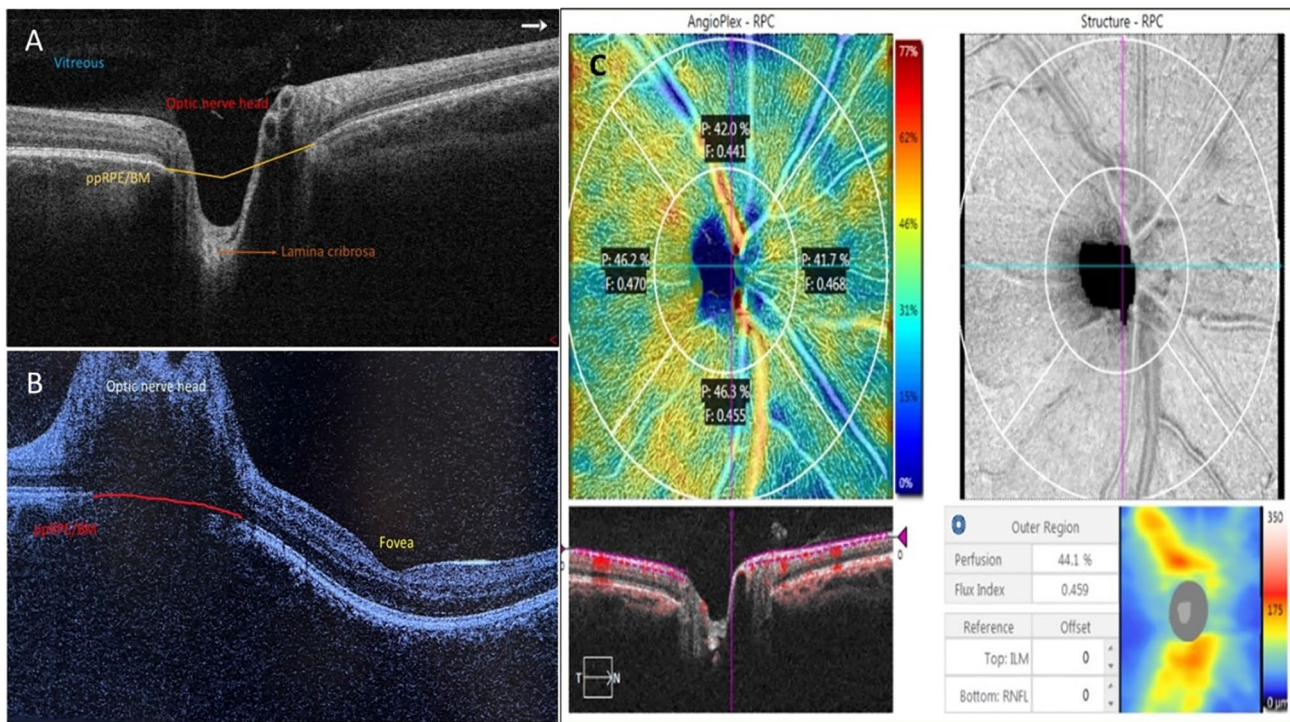


Fig. 4 **A** Optical coherence tomography (OCT) image of the optic nerve head. In healthy individuals, the peripapillary retinal pigment epithelium-basement membrane (ppRPE/BM) is V-shaped and angled away from the vitreous. **B** Optical coherence tomography (OCT)

image of the optic nerve head showing a U-shape configuration of the peripapillary retinal pigment epithelium-basement layer (ppRPE/BM) in a patient with papilledema. **C** Optical coherence tomography angiography (OCT-A) image of the optic nerve head

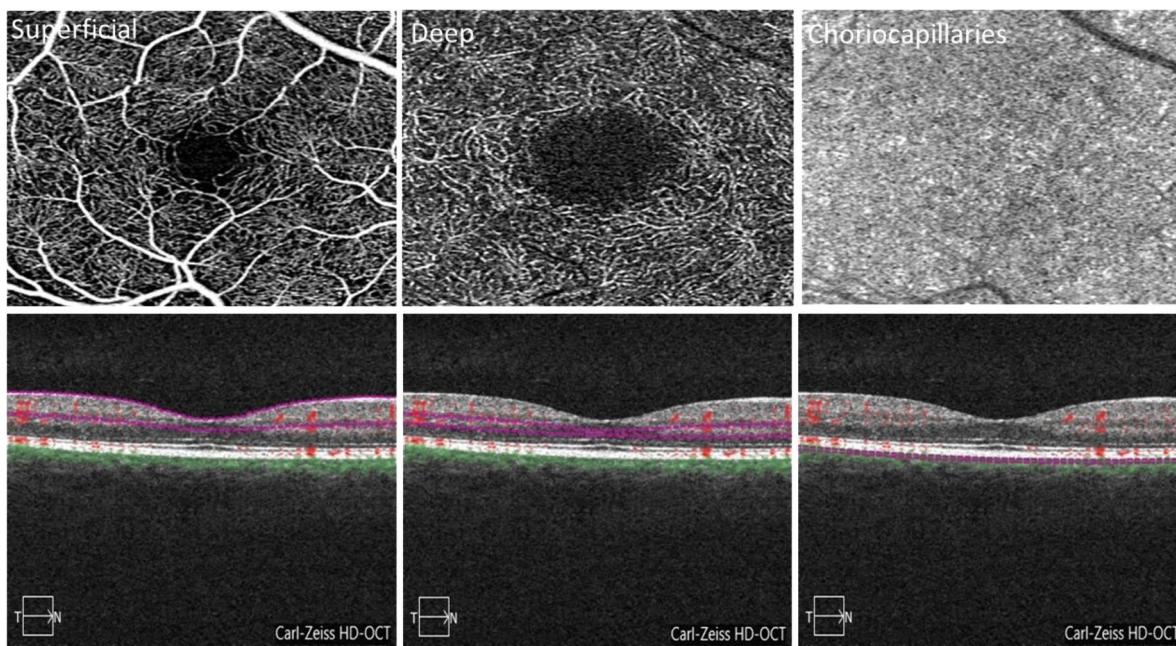


Fig. 5 Optical coherence tomography angiography (OCT-A) image displays the segmentation of three capillary plexus, including superficial, deep, and choriocapillaries, both in en face (top row) and

cross-sectional (bottom row). The segmentation boundaries for each layer are indicated by a pink line on the cross-sectional OCT-A image

et al. found a significant reduction in peripapillary vessel density among IHH patients compared to controls in their study using the AngioVue OCT-A device, which exclusively reported peripapillary vessel density (both global and sectoral). [107] Similarly, Cakir et al., utilizing Topcon imaging, observed a notable decrease in peripapillary vessel density across different retinal capillary plexus (SCP, DCP, and choriocapillaries) in IHH patients compared to controls [108]. However, Kaya et al., also using AngioVue reported a significant elevation in peripapillary vessel density in IHH patients compared to controls, offering a contradictory perspective [109]. In contrast, Fard et al., employing AngioVue found no significant difference in peripapillary capillary density between papilledema patients and controls [110]. Moreover, microvascular densities showed an increase in the nerve fiber layer plexus (NFLP) but a reduction in the SCP and DCP in IHH patients compared to controls using the Svision imaging OCT-A device [111]. Chonsui et al. in their study using PLEX Elite device showed a decreased peripapillary capillary density without changes in capillary flux intensity in eyes with papilledema [112].

Wang et al. in their study using AngioVue device showed that NFLP positively correlated with Frisén scores of patients with IHH [111]. However, SVP, IP, and DCP inversely correlated with Frisén scores of patients with IHH. Similarly, Pahuja et al. showed a negative correlation between superficial peripapillary retinal vessel perfusion and grades of papilledema using the Angioplex device (reported superficial capillary retinal vessel perfusion, deep retinal vessel perfusion and peripapillary choriocapillary perfusion) [102]. Kwapong et al. showed microvascular densities (superficial vascular complex and deep vascular complex) positively correlated with ICP using the Svision OCT-A device [113]. Peripapillary capillary vessel density in DCP was significantly reduced in optic disc edema compared to the control group, a condition that can mimic IHH. [108]

Discussion

OCT and OCT-A are non-invasive imaging methods widely used in ophthalmology to provide high-resolution cross-sectional images of the retina [114, 115]. OCT and OCT-A measurements have also shown to be a reliable indicator of neuronal death in various neurological disorders such as Parkinson's disease, Alzheimer's disease, multiple sclerosis, neuromyelitis optica, and spinocerebellar ataxia [116–119]. This systematic review examined existing literature to assess the effectiveness of OCT/OCT-A as a diagnostic and monitoring modality for IHH. The predominant imaging technique in the reviewed studies was OCT, with only ten studies using OCT-A. Among studies using OCT as the imaging modality for IHH patients, the most frequently assessed parameter was

RNFL thickness. Conversely, studies employing OCT-A as the imaging modality for IHH patients predominantly focused on peripapillary vessel density. In summary, studies utilizing OCT revealed increased thickness in RNFL, retina, as well as increased measurements in optic nerve head volume, optic nerve head height, optic disc diameter, rim area, and rim thickness. However, studies that used OCT-A as the imaging modality showed conflicting results regarding the peripapillary vessel density.

The RNFL comprises axons originating from retinal ganglion cells that converge from the retina and macular region to form the optic nerve. The RNFL is visualized in OCT images as the inner most retinal layer beneath the internal limiting membrane (Fig. 2). The peripapillary RNFL is measured along a 3 mm diameter circle centered on the optic nerve head and the mean thickness of the upper retinal layer is then presented as the average RNFL thickness (Fig. 6). The increased RNFL thickness reported in individuals with IHH is due to the disruption of the axonal transport and intraneural optic nerve sheath ischemia caused by the elevated CSF pressure in the subarachnoid space surrounding the optic nerve. Conversely, the reported decrease in macular GCC thickness in IHH patients is due to the loss of nerve fibers and retinal ganglion cells resulting from oxidative stress-associated prolonged swelling. The subarachnoid space connected to the optic nerve sheath undergoes structural changes due to alterations in the translaminal pressure gradient (difference between intraocular pressure and CSF pressure). Elevated ICP compresses the retrolaminar optic nerve and peripapillary scleral flange, causing deformation of the ppRPE/BM and adjacent sclera toward the vitreous [120–122]. Studies in this review have shown that in IHH patients, the configuration of the ppRPE/BM follows a U-shaped pattern around the optic nerve head, transitioning to a V-shape after interventions to lower CSF levels [19].

The earliest finding of raised ICP is optic disc swelling which takes about a week or 10 days to appear. However various diagnostic methods such as MRI, serum hormonal assay, axial length evaluation, pattern electroretinogram (PERG), and visually evoked potential (VEP) tests, can aid in detecting subclinical IHH. Liu et al. demonstrated that patients experiencing pulsatile tinnitus displayed several ocular and intracranial signs of IHH on MRI scans, such as optic nerve sheath enlargement, optic nerve tortuosity, posterior globe flattening, empty Sella, downward displacement of cerebellar tonsils into the foramen magnum, and slit-like lateral ventricles [123]. According to a study by Prabhat and colleagues, hormonal abnormalities such as raised prolactin, decreased TSH, and decreased cortisol were found in 37.5% of patients with IHH [124]. Moreover, studies have shown that the mean PERG and VEP amplitudes were reduced in IHH patients compared to healthy individuals [125]. Madill et al. in their study reported

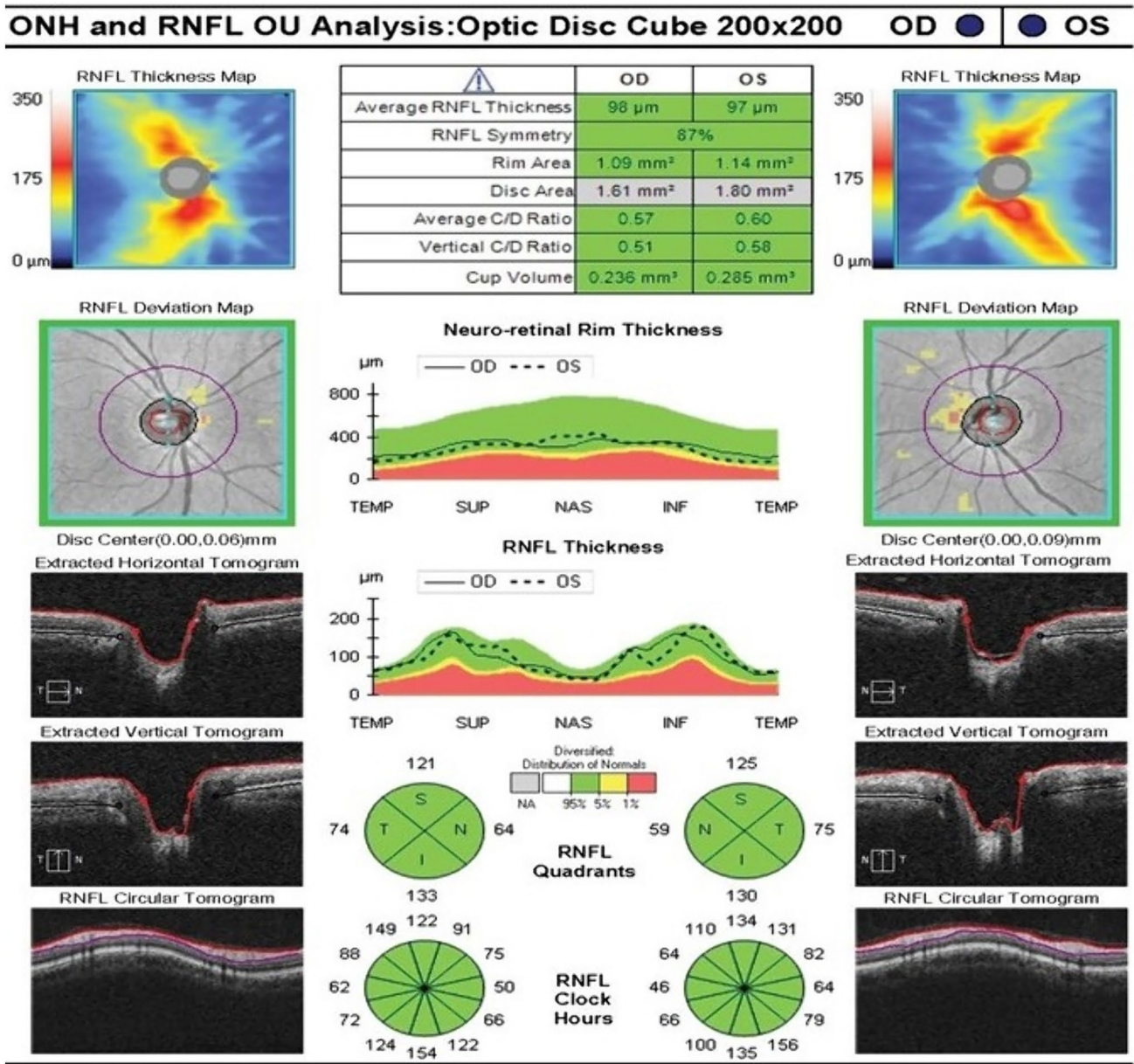


Fig. 6 Optical coherence tomography (OCT) test results showing optic nerve head (ONH) and retinal nerve fibre layer (RNFL) thickness of right (OD) and left eye (OS)

a significant difference in globe shape and axial length between patients with IIH and control subjects [126].

Swelling of the optic disc and increased thickness of the RNFL are not exclusive indicators of IIH or increased ICP because they can also occur in other optic neuropathies like optic neuritis and AION. Nevertheless, various parameters that describe the shape of the optic nerve head, such as, optic nerve head volume, optic nerve cup volume, central optic nerve head thickness, volume of Bruch’s membrane opening region, bending energy, minimal rim width of Bruch’s membrane opening (BMO-MRW), surface area of

BMO-MRW, and area of Bruch’s membrane opening, may aid in distinguishing between different optic neuropathies. In a study by Yadav et al., a 3D model of the optic nerve head was constructed using high-resolution OCT volume scans, and it was demonstrated that all of the aforementioned parameters, except for bending energy, exhibited differences between IIH, healthy controls, and optic neuritis [127]. Similarly, Kaufhold and colleagues employed volume scans to gauge optic nerve head volume in their study, revealing that 3D parameters such as optic nerve head volume and height could distinguish between IIH patients and controls [35].

These parameters were shown to be elevated in IIH patients even when the RNFL showed normal thickness, suggesting that it could serve as a potential marker of treatment efficacy and disease advancement [35]. Future studies employing OCT as a diagnostic tool for IIH could utilize the 3D optic nerve head parameters to differentiate IIH from other optic neuropathies such as glaucoma, optic neuritis, and AION.

The central retinal artery and ophthalmic artery traverse through the subarachnoid space and are influenced by changes in ICP [128]. Out of ten studies utilizing OCT-A as an imaging modality in IIH, five revealed a decrease in peripapillary vessel density [107, 108, 111–113], one demonstrated an increase in vessel density [109], and one found no disparity in vessel density between IIH patients and controls [110]. The decrease in vessel density seen in OCT-A can be due to mechanical compression of the capillary network caused by elevated ICP [129] or due to artifacts arising from the shadowing effect of fluid in papilledema artificially leading to decreased capillary density [129, 130]. Reduction in capillary vessel density has also been reported in other acute and chronic optic neuropathies such as optic neuritis, Leber's hereditary optic neuropathy (LHON), optic atrophy and non-arteritic anterior ischemic optic neuropathy (NAION) [39]. In cases of optic neuritis and dominant optic atrophy, the decrease in vessel density may result from reduced metabolic demands caused by neuronal degeneration and the atrophy of the peripapillary RNFL and GC-IPL, which subsequently reduces blood flow through autoregulatory mechanisms [131]. However, LHON is a peripapillary

microangiopathy that affects the endothelial and smooth muscle components of the blood vessel walls causing a significant reduction in the peripapillary capillary density [132]. In NAION, ischemic alterations due to dysfunctional vascular autoregulation may lead to the destruction of the capillaries [39].

The OCT parameters such as RNFL thickness, macular GCC thickness, rim area, disc area, and cup volume are easily obtained through device software (Figs. 6 and 7). However, certain parameters like optic nerve head volume, optic nerve head height, optic nerve head shape, peripapillary Bruch's membrane angle, anterior laminar surface depth, posterior laminar surface depth, and Bruch's membrane opening require manual calculation using custom segmentation algorithms. Most OCT devices do not automatically provide these measures, limiting their practicality in routine clinical use. In addition, accurately segmenting the outer retinal boundary in the presence of papilledema can be challenging and may lead to inaccuracies [133]. Another crucial OCT parameter for distinguishing papilledema in IIH from optic disc edema caused by other factors is the ppRPE/BM shape changes. These changes have shown a correlation with ICP [96]. However, the practical application of using ppRPE/BM changes in guiding clinical therapy is hindered by the lack of a commercial method and the need for extensive image processing to identify the RPE/BM boundary beneath an enlarged optic nerve head, limiting the integration of ppRPE/BM changes into clinical decision-making. OCT-A is relatively newer imaging methods offering both

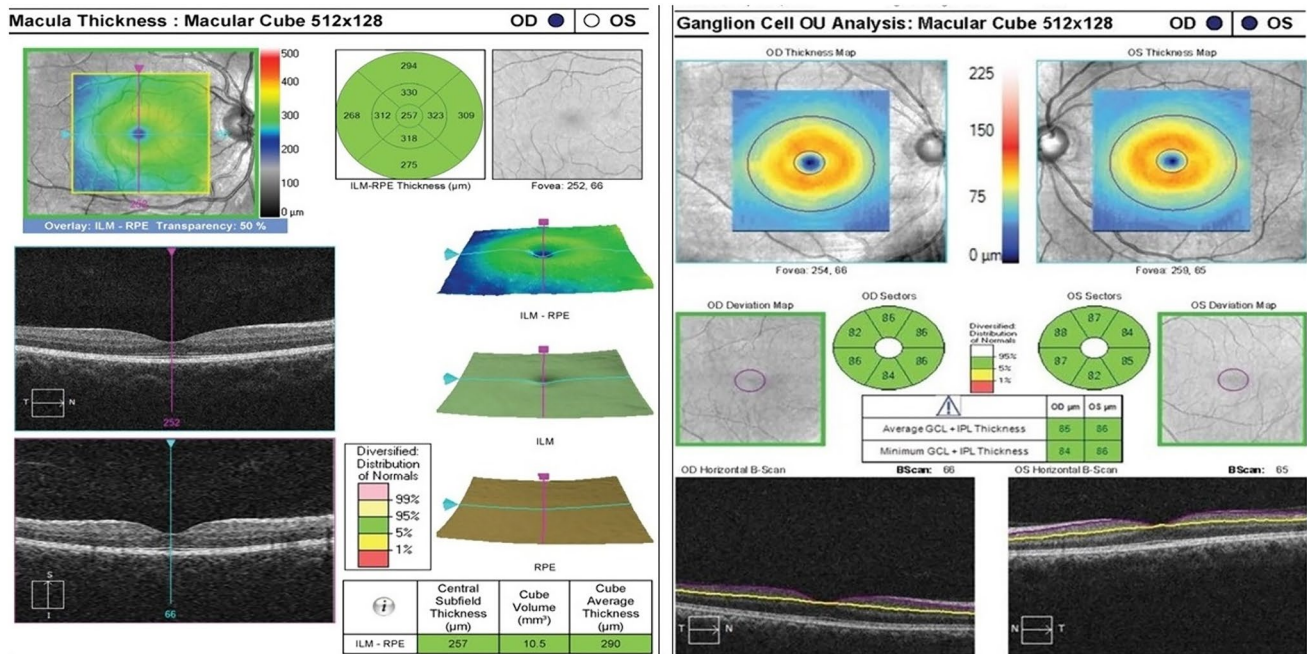


Fig. 7 Optical coherence tomography (OCT) imaging test results showing A, macular thickness and B, ganglion cell complex (GCC) thickness

structural and blood flow information within the retina and the choroid [134]. Given that recent studies using OCT-A in IHH have produced inconsistent findings regarding peripapillary vessel density, future research should concentrate on changes in the perifoveal capillary network. This is because IHH is linked to reduced blood flow in the ophthalmic and central retinal arteries [135].

This is the first systematic review to explore studies utilizing ocular imaging as a biomarker for IHH. One of the strengths is that it included 84 studies that used either OCT or OCT-A as the imaging modality in IHH patients. In addition, this systematic review employed study quality assessment tools to appraise the quality of the included studies. There were some limitations in the study. Most of the studies included in this review were case–control studies, with only two randomized control trials. This is because most studies focused on comparing the retinal and optic nerve head changes between IHH patients and healthy controls, thus adopting a case–control design. Another limitation of the study was that it only reviewed various OCT/OCT-A parameters in IHH and could not perform a meta-analysis of these common parameters. This initial step was necessary to understand the current studies and their reporting methods, which will facilitate future meta-analyses. Moreover, conducting a meta-analysis was not possible at this stage given the following reasons: (1) the studies had significantly different designs, methods, and levels of rigor, it might be inappropriate or misleading to statistically combine their results, (2) the outcomes were reported in diverse ways, making it difficult to aggregate the results meaningfully, and (3) some studies lacked sufficient data points for a robust meta-analysis, and some were of low quality or had a high risk of bias, which could lead to misleading conclusions if combined. A narrative approach allows for a more nuanced discussion of the quality and implications of each study. Finally, the specific research question or objective of the review was thought to be better addressed through a narrative synthesis, particularly because the question is broad or exploratory in nature. Another limitation was that our review comprised just ten studies examining the utility of OCT-A in individuals with IHH. This limited number of studies may be attributed to the fact that OCT-A is a relatively recent technology, and its effectiveness in a systemic condition like IHH has yet been firmly established.

To conclude, several OCT parameters have been demonstrated to be different in IHH patients compared to controls and retinal imaging may be useful as an efficient, non-invasive, and affordable biomarker for IHH patients.

Supplementary Information The online version contains supplementary material available at <https://doi.org/10.1007/s00415-024-12481-3>.

Author contributions All authors contributed to the study design and conceptualization. Mallika Prem Senthil and Jose Estevez

Bordon conducted the literature search. Mallika Prem Senthil, Ranjay Chakraborty, Paul Constable, Shannon Brown, and Simu Simon did the data curation and analysis. The risk of bias assessment was done by Saumya Anand and Dalia Al-Dasooqi. The initial manuscript draft was written by Mallika Prem Senthil with input from all authors on previous versions. All authors reviewed and endorsed the final manuscript.

Funding Open Access funding enabled and organized by CAUL and its Member Institutions. This study was not funded by any specific funding agencies.

Data availability The data supporting the findings of this systematic review can be obtained from the corresponding author, Mallika Prem Senthil on request.

Declarations

Conflicts of interest No potential conflict of interest was reported by the authors.

Open Access This article is licensed under a Creative Commons Attribution 4.0 International License, which permits use, sharing, adaptation, distribution and reproduction in any medium or format, as long as you give appropriate credit to the original author(s) and the source, provide a link to the Creative Commons licence, and indicate if changes were made. The images or other third party material in this article are included in the article's Creative Commons licence, unless indicated otherwise in a credit line to the material. If material is not included in the article's Creative Commons licence and your intended use is not permitted by statutory regulation or exceeds the permitted use, you will need to obtain permission directly from the copyright holder. To view a copy of this licence, visit <http://creativecommons.org/licenses/by/4.0/>.

References

1. Markey KA, Mollan SP, Jensen RH, Sinclair AJ (2016) Understanding idiopathic intracranial hypertension: mechanisms, management, and future directions. *Lancet Neurol* 15:78–91
2. Kesler A, Gadoth N (2001) Epidemiology of idiopathic intracranial hypertension in Israel. *J Neuroophthalmol* 21:12–14
3. Raouf N, Sharrack B, Pepper IM, Hickman SJ (2011) The incidence and prevalence of idiopathic intracranial hypertension in Sheffield, UK. *Eur J Neurol* 18:1266–1268
4. Durcan FJ, Corbett JJ, Wall M (1988) The incidence of pseudotumor cerebri. Population studies in Iowa and Louisiana. *Arch Neurol* 45:875–877
5. Craig JJ, Mulholland DA, Gibson JM (2001) Idiopathic intracranial hypertension; incidence, presenting features and outcome in Northern Ireland (1991–1995). *Ulster Med J* 70:31–35
6. Friesner D, Rosenman R, Lobb BM, Tanne E (2011) Idiopathic intracranial hypertension in the USA: the role of obesity in establishing prevalence and healthcare costs. *Obes Rev* 12:e372–380
7. Jacobson DM, Karanjia PN, Olson KA, Warner JJ (1990) Computed tomography ventricular size has no predictive value in diagnosing pseudotumor cerebri. *Neurology* 40:1454–1455
8. Bercaw BL, Greer M (1970) Transport of intrathecal 131-I risa in benign intracranial hypertension. *Neurology* 20:787–790
9. Riggeal BD, Bruce BB, Saindane AM, Ridha MA, Kelly LP, Newman NJ, Biousse V (2013) Clinical course of idiopathic intracranial hypertension with transverse sinus stenosis. *Neurology* 80:289–295
10. Giuseffi V, Wall M, Siegel PZ, Rojas PB (1991) Symptoms and disease associations in idiopathic intracranial hypertension

- (pseudotumor cerebri): a case–control study. *Neurology* 41:239–244
11. Wall M, George D (1991) Idiopathic intracranial hypertension. A prospective study of 50 patients. *Brain* 114(Pt 1A):155–180
 12. Mulla Y, Markey KA, Woolley RL, Patel S, Mollan SP, Sinclair AJ (2015) Headache determines quality of life in idiopathic intracranial hypertension. *J Headache Pain* 16:521
 13. Digre KB, Bruce BB, McDermott MP, Galetta KM, Balcer LJ, Wall M (2015) Quality of life in idiopathic intracranial hypertension at diagnosis: IIH treatment trial results. *Neurology* 84:2449–2456
 14. Wall M, Kupersmith MJ, Kiebertz KD, Corbett JJ, Feldon SE, Friedman DI, Katz DM, Keltner JL, Schron EB, McDermott MP (2014) The idiopathic intracranial hypertension treatment trial: clinical profile at baseline. *JAMA Neurol* 71:693–701
 15. Sadun AA, Currie JN, Lessell S (1984) Transient visual obscurations with elevated optic discs. *Ann Neurol* 16:489–494
 16. Lueck C, McIlwaine G (2005) Interventions for idiopathic intracranial hypertension. *Cochrane Database Syst Rev*. <https://doi.org/10.1002/14651858.CD003434.pub2>
 17. Bioussé V, Bruce BB, Newman NJ (2012) Update on the pathophysiology and management of idiopathic intracranial hypertension. *J Neurol Neurosurg Psychiatry* 83:488–494
 18. Smith M (2008) Monitoring intracranial pressure in traumatic brain injury. *Anesth Analg* 106:240–248
 19. Sibony P, Kupersmith MJ, Honkanen R, Rohlf FJ, Torab-Parhiz A (2014) Effects of lowering cerebrospinal fluid pressure on the shape of the peripapillary retina in intracranial hypertension. *Invest Ophthalmol Vis Sci* 55:8223–8231
 20. Saladino A, White JB, Wijidicks EF, Lanzino G (2009) Malplacement of ventricular catheters by neurosurgeons: a single institution experience. *Neurocrit Care* 10:248–252
 21. Gardner PA, Engh J, Atteberry D, Moosy JJ (2009) Hemorrhage rates after external ventricular drain placement. *J Neurosurg* 110:1021–1025
 22. Raboel PH, Bartek J Jr, Andresen M, Bellander BM, Romner B (2012) Intracranial pressure monitoring: invasive versus non-invasive methods—a review. *Crit Care Res Pract* 2012:950393
 23. Tran K, Pakzad-Vaezi K (2018) Multimodal imaging of diabetic retinopathy. *Curr Opin Ophthalmol* 29:566–575
 24. Le P, Zehden J, Zhang AY (2021) Role of optical coherence tomography angiography imaging in patients with diabetes. *Curr Diab Rep* 21:42
 25. Schimel AM, Fisher YL, Flynn HW Jr (2011) Optical coherence tomography in the diagnosis and management of diabetic macular edema: time-domain versus spectral-domain. *Ophthalm Surg Lasers Imaging* 42(Suppl):S41–55
 26. Regatieri CV, Branchini L, Duker JS (2011) The role of spectral-domain OCT in the diagnosis and management of neovascular age-related macular degeneration. *Ophthalm Surg Lasers Imaging* 42(Suppl):S56–66
 27. Talks SJ, Aftab AM, Ashfaq I, Soomro T (2017) The role of new imaging methods in managing age-related macular degeneration. *Asia Pac J Ophthalmol (Phil)* 6:498–507
 28. Hirano Y, Suzuki N, Tomiyasu T, Kurobe R, Yasuda Y, Esaki Y, Yasukawa T, Yoshida M, Ogura Y (2021) Multimodal imaging of microvascular abnormalities in retinal vein occlusion. *J Clin Med* 10:405
 29. Coffey AM, Hutton EK, Combe L, Bhindi P, Gertig D, Constable PA (2021) Optical coherence tomography angiography in primary eye care. *Clin Exp Optom* 104:3–13
 30. Wang JK, Kardon RH, Ledolter J, Sibony PA, Kupersmith MJ, Garvin MK (2017) Peripapillary retinal pigment epithelium layer shape changes from acetazolamide treatment in the idiopathic intracranial hypertension treatment trial. *Invest Ophthalmol Vis Sci* 58(5):2554–2565
 31. Anand A, Pass A, Urfy MZ, Tang R, Cajavilca C, Calvillo E, Suarez JI, Venkatasubba Rao CP, Bershada EM (2016) Optical coherence tomography of the optic nerve head detects acute changes in intracranial pressure. *J Clin Neurosci* 29:73–76
 32. Sarac O, Tasci YY, Gurdal C, Can I (2012) Differentiation of optic disc edema from optic nerve head drusen with spectral-domain optical coherence tomography. *J Neuroophthalmol* 32:207–211
 33. Carta A, Mora P, Aldigeri R, Gozzi F, Favilla S, Tedesco S, Calzetti G, Farci R, Barboni P, Bianchi-Marzoli S, Fossarello M, Gandolfi S, Sadun AA (2018) Optical coherence tomography is a useful tool in the differentiation between true edema and pseudoedema of the optic disc. *PLoS ONE* 13:e0208145
 34. Auinger P et al (2015) Papilledema outcomes from the optical coherence tomography substudy of the idiopathic intracranial hypertension treatment trial. *Ophthalmology* 122:1939–1945. e1932
 35. Kaufhold F, Kadas EM, Schmidt C, Kunte H, Hoffmann J, Zimmermann H, Oberwahrenbrock T, Harms L, Polthier K, Brandt AU, Paul F (2012) Optic nerve head quantification in idiopathic intracranial hypertension by spectral domain OCT. *PLoS ONE* 7:e36965
 36. Sibony P, Kupersmith MJ, Rohlf FJ (2011) Shape analysis of the peripapillary RPE layer in papilledema and ischemic optic neuropathy. *Invest Ophthalmol Vis Sci* 52:7987–7995
 37. Kupersmith MJ, Sibony PA, Feldon SE, Wang JK, Garvin M, Kardon R (2017) The effect of treatment of idiopathic intracranial hypertension on prevalence of retinal and choroidal folds. *Am J Ophthalmol* 176:77–86
 38. Sibony PA, Kupersmith MJ (2016) “Paton’s folds” revisited: peripapillary wrinkles, folds, and creases in papilledema. *Ophthalmology* 123:1397–1399
 39. Ghasemi Falavarjani K, Tian JJ, Akil H, Garcia GA, Sadda SR, Sadun AA (2016) Swept-source optical coherence tomography angiography of the optic disk in optic neuropathy. *Retina* 36(Suppl 1):S168–s177
 40. Rebolleda G, Munoz-Negrete FJ (2009) Follow-up of mild papilledema in idiopathic intracranial hypertension with optical coherence tomography. *Invest Ophthalmol Vis Sci* 50:5197–5200
 41. Waisbourd M, Leibovitch I, Goldenberg D, Kesler A (2011) OCT assessment of morphological changes of the optic nerve head and macula in idiopathic intracranial hypertension. *Clin Neurol Neurosurg* 113:839–843
 42. Marzoli SB, Ciasca P, Curone M, Cammarata G, Melzi L, Criscuoli A, Bussone G, D’Amico D (2013) Quantitative analysis of optic nerve damage in idiopathic intracranial hypertension (IIH) at diagnosis. *Neurol Sci* 34(Suppl 1):S143–145
 43. Skau M, Yri H, Sander B, Gerds TA, Milea D, Jensen R (2013) Diagnostic value of optical coherence tomography for intracranial pressure in idiopathic intracranial hypertension. *Graefes Arch Clin Exp Ophthalmol* 251:567–574
 44. Fard MA, Fakhree S, Abdi P, Hassanpoor N, Subramanian PS (2014) Quantification of peripapillary total retinal volume in pseudopapilledema and mild papilledema using spectral-domain optical coherence tomography. *Am J Ophthalmol* 158:136–143
 45. Starks V, Gilliland G, Vrcek I, Gilliland C (2016) Effect of optic nerve sheath fenestration for idiopathic intracranial hypertension on retinal nerve fiber layer thickness. *Orbit* 35:87–90
 46. Dinkin MJ, Patsalides A (2017) Venous sinus stenting in idiopathic intracranial hypertension: results of a prospective trial. *J Neuroophthalmol* 37:113–121
 47. Saenz R, Cheng H, Prager TC, Frishman LJ, Tang RA (2017) Use of A-scan ultrasound and optical coherence tomography to differentiate papilledema from pseudopapilledema. *Optom Vis Sci* 94:1081–1089

48. Aojula A, Mollan SP, Horsburgh J, Yiangou A, Markey KA, Mitchell JL, Scotton WJ, Keane PA, Sinclair AJ (2018) Segmentation error in spectral domain optical coherence tomography measures of the retinal nerve fibre layer thickness in idiopathic intracranial hypertension. *BMC Ophthalmol* 17:257
49. Huang-Link Y, Eleftheriou A, Yang G, Johansson JM, Apostolou A, Link H, Jin YP (2019) Optical coherence tomography represents a sensitive and reliable tool for routine monitoring of idiopathic intracranial hypertension with and without papilledema. *Eur J Neurol* 26:808–e857
50. Onder H, Erkan E (2019) The association of optical coherence tomography results with neuroimaging signs and some clinical parameters in idiopathic intracranial hypertension. *J Neurol Res* 9:65–71
51. Merticariu CI, Balta F, Merticariu A, Ciuluvica R, Voinea L (2019) Optical coherence tomography assessment of structural changes in the optic nerve head and peripapillary retina in idiopathic intracranial hypertension. *Arch Balk Med Union* 54:267–273
52. Wall M, Subramani A, Chong LX, Galindo R, Turpin A, Kardon RH, Thurtell MJ, Bailey JA, Marin-Franch I (2019) Threshold static automated perimetry of the full visual field in idiopathic intracranial hypertension. *Invest Ophthalmol Vis Sci* 60:1898–1905
53. Bahnasy WS, El-Heneedy YAE, Elhassanien MEM, Sharaf AF, Khalid HA (2019) Neuro-ophthalmological biomarkers of visual outcome in newly diagnosed idiopathic intracranial hypertension. *Egypt J Neurol Psychiatry Neurosurg* 55:26
54. Flowers AM, Longmuir RA, Liu Y, Chen Q, Donahue SP (2021) Variability within optic nerve optical coherence tomography measurements distinguishes papilledema from pseudopapilledema. *J Neuroophthalmol* 41(4):496–503
55. Carey AR, Bosley TM, Miller NR, McCulley TJ, Henderson AD (2021) Use of en face optical coherence tomography to monitor papilledema in idiopathic intracranial hypertension: a pilot study. *J Neuroophthalmol* 41:212–216
56. Kohli AA, Pistilli M, Alfaro C, Ross AG, Jivraj I, Bagchi S, Chan J, May D, Liu GT, Shindler KS, Tamhankar MA (2021) Role of ocular ultrasonography to distinguish papilledema from pseudopapilledema. *J Neuroophthalmol* 41:206–211
57. Inam ME, Martinez-Gutierrez JC, Kole MJ, Sanchez F, Lekka E, Truong VTT, Lopez-Rivera V, Sheriff FG, Zima LA, Pedroza C, Tang R, Adesina OO, Engstrom A, Sheth SA, Chen PR (2022) Venous sinus stenting for low pressure gradient stenoses in idiopathic intracranial hypertension. *Neurosurgery* 91:734–740
58. Thaller M, Tsermoulas G, Sun R, Mollan SP, Sinclair AJ (2021) Negative impact of COVID-19 lockdown on papilloedema and idiopathic intracranial hypertension. *J Neurol Neurosurg Psychiatry* 92:795–797
59. Sood G, Samanta R, Kumawat D, Agrawal A, Singh A (2022) Clinical profile and retinal nerve fibre layer thickness of optic disc oedema patients at a tertiary care institute in North India. *Therapy* 14:25158414211072630
60. Vosoughi AR, Margolin EA, Micieli JA (2022) Idiopathic intracranial hypertension: incidental discovery versus symptomatic presentation. *J Neuroophthalmol* 42:187–191
61. Kaya Tutar N, Kale N (2023) The relationship between lumbar puncture opening pressure and retinal nerve fiber layer thickness in the diagnosis of idiopathic intracranial hypertension: is a lumbar puncture always necessary? *Neurolog* 25:25
62. Xie JS, Donaldson L, Margolin EA (2023) Swelling of atrophic optic discs in idiopathic intracranial hypertension. *J Neuroophthalmol* 44(2):212–218
63. Srijja YN, Pattnaik L, Mishra S, Panigrahi PK (2024) An optical coherence study on optic disc parameters and peripapillary retinal nerve fiber layer thickness in patients with optic disc edema. *Indian J Ophthalmol* 72:S96–S100
64. Jensen R, Skau M (2010) Disease activity in idiopathic intracranial hypertension: a 3-month follow-up study. *J Headache Pain* 1:S71
65. Scott CJ, Kardon RH, Lee AG, Frisen L, Wall M (2010) Diagnosis and grading of papilledema in patients with raised intracranial pressure using optical coherence tomography vs clinical expert assessment using a clinical staging scale. *Arch Ophthalmol* 128:705–711
66. Skau M, Sander B, Milea D, Jensen R (2011) Disease activity in idiopathic intracranial hypertension: a 3-month follow-up study. *J Neurol* 258:277
67. Yri HM, Jensen RH (2015) Idiopathic intracranial hypertension: clinical nosography and field-testing of the ICHD diagnostic criteria. A case-control study. *Cephalalgia* 35:553–562
68. Auinger P, Durbin M, Feldon S, Garvin M, Kardon R, Keltner J, Kupersmith M, Sibony P, Plumb K, Wang JK, Werner JS (2014) Baseline OCT measurements in the idiopathic intracranial hypertension treatment trial, part I: quality control, comparisons, and variability. *Invest Ophthalmol Vis Sci* 55:8180–8188
69. Bingol Kiziltunc P, Atilla H (2021) A novel biomarker for increased intracranial pressure in idiopathic intracranial hypertension. *Jpn J Ophthalmol* 65(3):416–422
70. Attia R, Fitoussi R, Mairot K, Demortiere S, Stellman JP, Tilsley P, Audoin B, David T, Stolowy N (2023) Risk factors associated with progression from papilloedema to optic atrophy: results from a cohort of 113 patients. *BMJ Open Ophthalmol* 8:e001375
71. Wang JR, Linton EF, Johnson BA, Kupersmith MJ, Garvin MK, Kardon RH (2024) Visualization of optic nerve structural patterns in papilledema using deep learning variational autoencoders. *Transl Vis Sci Technol* 13:13
72. Monteiro ML, Afonso CL (2014) Macular thickness measurements with frequency domain-OCT for quantification of axonal loss in chronic papilledema from pseudotumor cerebri syndrome. *Eye* 28:390–398
73. Goldhagen BE, Bhatti MT, Srinivasan PP, Chiu SJ, Farsiou S, El-Dairi MA (2015) Retinal atrophy in eyes with resolved papilledema detected by optical coherence tomography. *J Neuroophthalmol* 35:122–126
74. Kabatas N, Eren Y, Nalcacioglu P, Caliskan S, Bicer T, Comoglu SS, Gurdal C (2021) Management of the regression of papilledema with regional axon loss in idiopathic intracranial hypertension patients. *Int Ophthalmol* 41:1467–1477
75. Rehman O, Ichhpujani P, Singla E, Negi R, Kumar S (2022) Change in contrast sensitivity and OCT parameters in idiopathic intracranial hypertension. *Ther Adv Ophthalmol* 14:25158414221083360
76. Chen JJ, Thurtell MJ, Longmuir RA, Garvin MK, Wang JK, Wall M, Kardon RH (2015) Causes and prognosis of visual acuity loss at the time of initial presentation in idiopathic intracranial hypertension. *Invest Ophthalmol Vis Sci* 56:3850–3859
77. Labib D, Abdel Raouf D (2015) Diagnostic value of optical coherence tomography in patients with idiopathic intracranial hypertension. *Egypt J Neurol Psychiatry Neurosurg* 52:249
78. Moss HE, Park JC, McAnany JJ (2015) The photopic negative response in idiopathic intracranial hypertension. *Invest Ophthalmol Vis Sci* 56:3709–3714
79. Park JC, Moss HE, McAnany JJ (2018) Electroretinography in idiopathic intracranial hypertension: comparison of the pattern ERG and the photopic negative response. *Doc Ophthalmol* 136:45–55
80. Chen Q, Feng C, Zhao G, Chen W, Wang M, Sun X, Sha Y, Li Z, Tian G (2020) Pseudotumour cerebri syndrome in China: a cohort study. *Sci Rep* 10:1222

81. Nogueira PF, Caiado GC, Gracitelli CPB, Martins FM, Barros FCD, Matas SLA, Teixeira SH, Noia LDC, Paulo DA (2021) Association between optical coherence tomography measurements and clinical parameters in idiopathic intracranial hypertension. *J Ophthalmol* 2021:1401609
82. Wibroe EA, Malmqvist L, Hamann S (2021) OCT based interpretation of the optic nerve head anatomy and prevalence of optic disc drusen in patients with idiopathic intracranial hypertension (IIH). *Life (Basel)* 11:584
83. Bassi ST, Pamu R, Ambika S, Praveen S, Priyadarshini D, Dharini V, Padmalakshmi K (2024) Optical coherence tomography in papilledema: a probe into the intracranial pressure correlation. *Indian J Ophthalmol* 62:1146–1151
84. Touzé R, Bonnin S, Houdart E, Nicholson P, Bodaghi B, Shotar E, Clarençon F, Lenck S, Touitou V (2021) Long-term kinetic papilledema improvement after venous sinus stenting in idiopathic intracranial hypertension. *Clin Neuroradiol* 31:483–490
85. Thaller M, Homer V, Mollan SP, Sinclair AJ (2023) Asymptomatic idiopathic intracranial hypertension: prevalence and prognosis. *Clin Exp Ophthalmol* 51:598–606
86. Albrecht P, Blasberg C, Ringelstein M, Müller AK, Finis D, Guthoff R, Kadas EM, Lagreze W, Aktas O, Hartung HP, Paul F, Brandt AU, Methner A (2017) Optical coherence tomography for the diagnosis and monitoring of idiopathic intracranial hypertension. *J Neurol* 264:1370–1380
87. Sheils CR, Fischer WS, Hollar RA, Blanchard LM, Feldon SE (2018) The relationship between optic disc volume, area, and Frisén score in patients with idiopathic intracranial hypertension. *Am J Ophthalmol* 195:101–109
88. Vijay V, Mollan SP, Mitchell JL, Bilton E, Alimajstorovic Z, Markey KA, Fong A, Walker JK, Lyons HS, Yiangou A, Tsermoulas G, Brock K, Sinclair AJ (2020) Using optical coherence tomography as a surrogate of measurements of intracranial pressure in idiopathic intracranial hypertension. *JAMA Ophthalmol* 138:1264–1271
89. Chang YC, Alperin N, Bagci AM, Lee SH, Rosa PR, Giovanni G, Lam BL (2015) Relationship between optic nerve protrusion measured by OCT and MRI and papilledema severity. *Invest Ophthalmol Vis Sci* 56:2297–2302
90. Eren Y, Kabatas N, Guven H, Comoglu S, Gurdal C (2019) Evaluation of optic nerve head changes with optical coherence tomography in patients with idiopathic intracranial hypertension. *Acta Neurol Belg* 119:351–357
91. Rehman O, Ichhpujani P, Kumar S, Saroa R, Sawal N (2022) Idiopathic intracranial hypertension and visual function in North Indian population. *Eur J Ophthalmol* 32(2):1186–1193
92. Kaya FS, Arici C (2023) Assessment of peripapillary choroidal thicknesses and optic disc diameters in idiopathic intracranial hypertension. *Can J Ophthalmol* 58:212–218
93. Sinclair AJ, Burdon MA, Nightingale PG, Ball AK, Good P, Matthews TD, Jacks A, Lawden M, Clarke CE, Stewart PM, Walker EA, Tomlinson JW, Rauz S (2010) Low energy diet and intracranial pressure in women with idiopathic intracranial hypertension: prospective cohort study. *BMJ* 341:c2701
94. Sibony PA, Kupersmith MJ, Feldon SE, Wang JK, Garvin M, Auinger P, Durbin M, Garvin MK, Kardon RH, Keltner J, Wang JK, Kupersmith M, Cello K, Werner JS (2015) Retinal and choroidal folds in papilledema. *Invest Ophthalmol Vis Sci* 56:5670–5680
95. Reggie SN, Avery RA, Bavinger JC, Jivraj I, Alfaro C, Pistilli M, Kohli AA, Liu GT, Shindler KS, Ross AG, Kardon RH, Sibony PA, Tamhankar M (2021) The sensitivity and specificity of retinal and choroidal folds to distinguish between mild papilloedema and pseudopapilledema. *Eye (Basingstoke)* 35(11):3131–3136
96. Gampa A, Vangipuram G, Shirazi Z, Moss HE (2017) Quantitative association between peripapillary Bruch's membrane shape and intracranial pressure. *Invest Ophthalmol Vis Sci* 58:2739–2745
97. Banik R, Kupersmith MJ, Wang JK, Garvin MK (2019) The effect of acetazolamide and weight loss on intraocular pressure in idiopathic intracranial hypertension patients. *J Glaucoma* 28:352–356
98. Panyala R, Sharma P, Sihota R, Saxena R, Prasad K, Phuljhele S, Gurralla S, Bhaskaran K (2021) Role of spectral domain optical coherence tomography in the diagnosis and prognosis of papilledema. *Indian J Ophthalmol* 69:2372–2377
99. Pasaoglu I, Satana B, Altan C, Artunay O, Basarir B, Onmez FE, Inal A (2019) Lamina cribrosa surface position in idiopathic intracranial hypertension with swept-source optical coherence tomography. *Indian J Ophthalmol* 67:1085–1088
100. Tatar IT, Solmaz B, Erdem ZG, Pasaoglu I, Demircan A, Tülü Aygün B, Ozkaya A (2020) Morphological assessment of lamina cribrosa in idiopathic intracranial hypertension. *Indian J Ophthalmol* 68:164–167
101. Ozdemir I, Çevik S (2020) Measurement of choroid thickness using optical coherence tomography to monitor intracranial pressure in an idiopathic cranial hypertension model. *Neurol India* 68:636–639
102. Pahuja A, Dhiman R, Aggarwal V, Aalok SP, Saxena R (2024) Evaluation of peripapillary and macular optical coherence tomography angiography characteristics in different stages of papilledema. *J Neuroophthalmol* 44:53–60
103. Dreesbach M, Joachimsen L, Kuchlin S, Reich M, Gross NJ, Brandt AU, Schuchardt F, Harloff A, Bohringer D, Lagreze WA (2020) Optic nerve head volumetry by optical coherence tomography in papilledema related to idiopathic intracranial hypertension. *Transl Vis Technol* 9:24
104. Lin Y, Chen S, Zhang M (2021) Peripapillary vessel density measurement of quadrant and clock-hour sectors in primary angle closure glaucoma using optical coherence tomography angiography. *BMC Ophthalmol* 21:328
105. Mansoori T, Balakrishna N (2019) Peripapillary vessel density and retinal nerve fiber layer thickness in patients with unilateral primary angle closure glaucoma with superior hemifield defect. *J Curr Glaucoma Pract* 13:21–27
106. Borrelli E, Parravano M, Sacconi R, Costanzo E, Querques L, Vella G, Bandello F, Querques G (2020) Guidelines on optical coherence tomography angiography imaging: 2020 focused update. *Ophthalmol Ther* 9:697–707
107. Tüntaş Bilen F, Atilla H (2019) Peripapillary vessel density measured by optical coherence tomography angiography in idiopathic intracranial hypertension. *J Neuroophthalmol* 39:319–323
108. Yalcinkaya Cakir G, Solmaz B, Cakir I, Pasaoglu IB, Taskapili M (2024) Optical coherence tomography angiography findings in optic disc drusen and idiopathic intracranial hypertension. *Eur J Ophthalmol* 34:566–573
109. Kaya FS, Sonbahar O, Açar PA, Özbaş M, Yigit FU (2021) Evaluating peripapillary vessel density in regressed papilledema in idiopathic intracranial hypertension patients. *Photodiagn Photodyn Ther* 36:102551
110. Fard MA, Sahraiyani A, Jalili J, Hejazi M, Suwan Y, Ritch R, Subramanian PS (2019) Optical coherence tomography angiography in papilledema compared with pseudopapilledema. *Invest Ophthalmol Vis Sci* 60:168–175
111. Wang H, Cao L, Kwapong WR, Liu G, Wang R, Liu J, Wu B (2023) Optic nerve head changes measured by swept source optical coherence tomography and angiography in patients with intracranial hypertension. *Ophthalmol Ther* 12:3295–3305
112. Chonsui M, Le Goff M, Korobelnik JF, Rougier MB (2022) Quantitative analysis of radial peripapillary capillary network in patients with papilledema compared with healthy subjects using

- optical coherence tomography angiography. *J Neuroophthalmol* 42:e109–e115
113. Kwapong WR, Cao L, Pan R, Wang H, Ye C, Tao W, Liu J, Wu B (2023) Retinal microvascular and structural changes in intracranial hypertension patients correlate with intracranial pressure. *CNS Neurosci Ther* 29:4093–4101
 114. Adhi M, Duker JS (2013) Optical coherence tomography—current and future applications. *Curr Opin Ophthalmol* 24:213–221
 115. Gabriele ML, Wollstein G, Ishikawa H, Kagemann L, Xu J, Folio LS, Schuman JS (2011) Optical coherence tomography: history, current status, and laboratory work. *Invest Ophthalmol Vis Sci* 52:2425–2436
 116. Ratchford JN, Quigg ME, Conger A, Frohman T, Frohman E, Balcer LJ, Calabresi PA, Kerr DA (2009) Optical coherence tomography helps differentiate neuromyelitis optica and MS optic neuropathies. *Neurology* 73:302–308
 117. Stricker S, Oberwahrenbrock T, Zimmermann H, Schroeter J, Endres M, Brandt AU, Paul F (2011) Temporal retinal nerve fiber loss in patients with spinocerebellar ataxia type 1. *PLoS ONE* 6:e23024
 118. Moschos MM, Tagaris G, Markopoulos I, Margetis I, Tsapakis S, Kanakis M, Koutsandrea C (2011) Morphologic changes and functional retinal impairment in patients with Parkinson disease without visual loss. *Eur J Ophthalmol* 21:24–29
 119. Petzold A, de Boer JF, Schipling S, Vermersch P, Kardon R, Green A, Calabresi PA, Polman C (2010) Optical coherence tomography in multiple sclerosis: a systematic review and meta-analysis. *Lancet Neurol* 9:921–932
 120. Burgoyne CF, Downs JC, Bellezza AJ, Suh JK, Hart RT (2005) The optic nerve head as a biomechanical structure: a new paradigm for understanding the role of IOP-related stress and strain in the pathophysiology of glaucomatous optic nerve head damage. *Prog Retin Eye Res* 24:39–73
 121. Bellezza AJ, Hart RT, Burgoyne CF (2000) The optic nerve head as a biomechanical structure: initial finite element modeling. *Invest Ophthalmol Vis Sci* 41:2991–3000
 122. Strouthidis NG, Fortune B, Yang H, Sigal IA, Burgoyne CF (2011) Effect of acute intraocular pressure elevation on the monkey optic nerve head as detected by spectral domain optical coherence tomography. *Invest Ophthalmol Vis Sci* 52:9431–9437
 123. Liu Z, Dong C, Wang X, Han X, Zhao P, Lv H, Li Q, Wang Z (2015) Association between idiopathic intracranial hypertension and sigmoid sinus dehiscence/diverticulum with pulsatile tinnitus: a retrospective imaging study. *Neuroradiology* 57:747–753
 124. Prabhat N, Kaur K, Takkar A, Ahuja C, Katoch D, Goyal M, Dutta P, Bhansali A, Lal V (2024) Pituitary dysfunction in idiopathic intracranial hypertension: an analysis of 80 patients. *Can J Neurol Sci* 51:265–271
 125. Falsini B, Tamburrelli C, Porciatti V, Anile C, Porrello G, Mangiola N (1992) Pattern electroretinograms and visual evoked potentials in idiopathic intracranial hypertension. *Ophthalmologica* 205:194–203
 126. Madill SA, Connor SE (2005) Computed tomography demonstrates short axial globe length in cases with idiopathic intracranial hypertension. *J Neuroophthalmol* 25:180–184
 127. Yadav SK, Kadas EM, Motamedi S, Polthier K, Haußer F, Gawlik K, Paul F, Brandt A (2018) Optic nerve head three-dimensional shape analysis. *J Biomed Opt* 23:1–13
 128. Mitra RA, Sergott RC, Flaharty PM, Lieb WE, Savino PJ, Bosley TM, Hedges TR Jr (1993) Optic nerve decompression improves hemodynamic parameters in papilledema. *Ophthalmology* 100:987–997
 129. Hayreh SS, Zimmerman MB (2008) Non-arteritic anterior ischemic optic neuropathy: role of systemic corticosteroid therapy. *Graefes Arch Clin Exp Ophthalmol* 246:1029–1046
 130. Sharma S, Ang M, Najjar RP, Sng C, Cheung CY, Rukmini AV, Schmetterer L, Milea D (2017) Optical coherence tomography angiography in acute non-arteritic anterior ischaemic optic neuropathy. *Br J Ophthalmol* 101:1045–1051
 131. Mohammadi S, Gouravani M, Salehi MA, Arevalo JF, Galetta SL, Harandi H, Frohman EM, Frohman TC, Saidha S, Sattarnejad N, Paul F (2023) Optical coherence tomography angiography measurements in multiple sclerosis: a systematic review and meta-analysis. *J Neuroinflamm* 20:85
 132. Borrelli E, Balasubramanian S, Triolo G, Barboni P, Satta SR, Sadun AA (2018) Topographic macular microvascular changes and correlation with visual loss in chronic leber hereditary optic neuropathy. *Am J Ophthalmol* 192:217–228
 133. Malhotra K, Padungkiatsagul T, Moss HE (2020) Optical coherence tomography use in idiopathic intracranial hypertension. *Ann Eye Sci* 5:7
 134. Spaide RF, Fujimoto JG, Waheed NK, Satta SR, Staurenghi G (2018) Optical coherence tomography angiography. *Prog Retin Eye Res* 64:1–55
 135. Querfurth HW, Lagrèze WD, Hedges TR, Heggerick PA (2002) Flow velocity and pulsatility of the ocular circulation in chronic intracranial hypertension. *Acta Neurol Scand* 105:431–440
 136. Skau M, Milea D, Sander B, Wegener M, Jensen R (2011) OCT for optic disc evaluation in idiopathic intracranial hypertension. *Graefes Arch Clin Exp Ophthalmol* 249:723–730
 137. Afonso CL, Raza AS, Kreuz AC, Hokazono K, Cunha LP, Oyamada MK, Monteiro ML (2015) Relationship between pattern electroretinogram, frequency-domain OCT, and automated perimetry in chronic papilledema from pseudotumor cerebri syndrome. *Invest Ophthalmol Vis Sci* 56:3656–3665
 138. Banerjee M, Phuljhele S, Saluja G, Kumar P, Saxena R, Sharma P, Vibha D, Pandit AK (2022) Optical coherence tomography features and correlation of functional and structural parameters in patients of idiopathic intracranial hypertension. *Indian J Ophthalmol* 70:1343–1349
 139. Thaller M, Homer V, Hyder Y, Yiangou A, Liczkowski A, Fong AW, Virdee J, Piccus R, Roque M, Mollan SP, Sinclair AJ (2023) The idiopathic intracranial hypertension prospective cohort study: evaluation of prognostic factors and outcomes. *J Neurol* 270:851–863
 140. Rodriguez Torres Y, Lee P, Mhlstin M, Tomsak RL (2021) Correlation between optic disc peripapillary capillary network and papilledema grading in patients with idiopathic intracranial hypertension: a study of optical coherence tomography angiography. *J Neuroophthalmol* 41:48–53
 141. El-Haddad N, Ismael SA, El-Wahab AA, Shalaby S, Farag MMA, Mohammd NS, Shawky S (2023) Optic disc vessel density changes after shunt surgery in idiopathic intracranial hypertension. *Photodiagn Photodyn Ther* 42:103625